Recognizing a lost nesting ground: First unambiguous Testudines eggshells from the Eocene, associated with the pleurodiran *Eocenochelus* (Huesca, Northern Spain)

Miguel Moreno-Azanza[a,b,c]*, Ester Díaz-Berenguer[c]*, Roi Silva-Casal[d], Adán Pérez-García[e], Ainara Badiola[f], José Ignacio Canudo[c]

[a] GeoBioTec, Department of Earth Sciences, NOVA School of Science and Technology, Campus de Caparica, P-2829 516 Caparica, Portugal. mmazanza@fct.unl.pt.

[b] Espaço NovaPaleo, Museu de Lourinhã, Rua João Luis de Moura 95, 2530-158, Lourinhã, Portugal.

[c] Grupo Aragosaurus-IUCA, Facultad de Ciencias, Universidad de Zaragoza, 50009, Zaragoza, Spain. ester.berenguer@gmail.com; jicanudo@unizar.es

[d]Institut de Recerca Geomodels, Universitat de Barcelona, Spain. roi.silva.casal@gmail.com

[e]Grupo de Biología Evolutiva, Facultad de Ciencias, UNED, 28040, Madrid, Spain. paleontologo@gmail.com

[f] Dpto. Geología, Facultad de Ciencia y Tecnología, Universidad del País Vasco (UPV/EHU), Barrio Sarriena s/n, 48940 Leioa, Spain. ainara.badiola@ehu.eus

***Corresponding authors**: E-mail address: mmazanza@fct.unl.pt (M. Moreno-Azanza); ester.berenger@gmail.com (E. Díaz-Berenguer)

Abstract

The Eocene record of turtle eggshells is scarce, with a single unconfirmed report from France. This scarcity contrasts with the great abundance of osteological remains, distributed

over a wide palaeogeographical range as a result of climatic warmth. In this paper, we describe the first definitive Eocene Testudoolithidae eggshell fragments attributable to Testudines, most likely pleurodiran turtles, from the Eocene Sobrarbe Formation at the Castejón de Sobrarbe fossil site (CS-41) in northern Spain. The eggshells were found in association with osteological remains of at least four individuals of *Eocenochelus eremberti* (Pleurodira, Erymnochelyini) in an otherwise sirenian-dominated bonebed. Analysis of eggshell ultra- and microstructure allows comparison with eggshells from fossil and extant turtles. The eggshells are highly recrystallized but preserve relics of their original aragonitic radial ultrastructure as crystal phantoms. The barrel-shaped shell units, which are taller than wide, with compactituberculate ornamentation and funnel-shaped pore openings are similar to those of the Palaeocene ootaxon *Haininchelys curiosa*, whose holotype and paratype have been lost. The CS-41 eggshells are most similar to those of the pleurodiran *Erymnochelys madagascariensis* from Madagascar, the closest living relative to *Eocenochelus*, further supporting our attribution. Sedimentological and taphonomic analysis of the assemblage supports the hypothesis that the CS-41 fossil site was formed as the infilling of an abandoned tributary channel in the deltaic plain by an overbank or debris-flow deposit associated with a storm event. This storm reworked the remains of a nesting ground of *Eocenochelus eremberti*, an otherwise coastal turtle, which would have entered inland streams to nest in the sand bars at the mouth of the Sobrarbe Deltaic Complex.

***Highlights**:*

- A mono-ootaxic assemblage of thousands of Testudoolithidae eggshell fragments is described from the Eocene of Spain
- They are the first unambiguous Testudines eggshells from the Eocene
- Eggshells are suggestive of a pleurodiran producer, and co-occur with *Eocenochelus eremberti* remains
- Eggs were probably laid in the sand bars of the delta mouth
- Eggs were exhumed, fragmented and redeposited in an abandoned channel in the deltaic plain following a storm

Keywords:

Testudoolithidae, eggshell taphonomy, Erymnochelyini, Sobrarbe Deltaic Complex; Lutetian

1. Introduction

The Eocene is a period that saw important changes in the climate directly reflected in the biota. It was a warm period during which the tropical belts stretched to high latitudes, a phenomenon that has been associated with the radiation and dispersion of many vertebrate groups (Bowen et al., 2002; Hooker, 1998; Gingerich, 2006; Solé and Smith, 2013). One of the groups that benefited from this climatic warming was the pleurodiran turtles, which are normally restricted to tropical latitudes, but which profited from the warmer ocean and continental waters to expand their palaeogeographical distribution significantly (Pérez-García, 2016; Pérez-García et al., 2017). During the Upper Cretaceous, pleurodires were very diverse in southwestern Europe. These turtles were represented by several lineages that reached Europe diachronically, becoming the most abundant form of turtles in the Upper Cretaceous freshwater and coastal ecosystems of the continent (see Pérez-García, 2017, 2018). However, current evidence suggests that they were completely absent in Europe during the Palaeocene, again reaching this continent at the beginning of the early Eocene, favoured by the afore-mentioned increase in temperatures resulting from the Palaeocene-Eocene Thermal Maximum (PETM, see Pérez-García, 2017, and references therein). Two lineages of Podocnemididae (a clade of pleurodiran turtles) are recognized in the Eocene record of Europe, represented by two genera exclusive to this continent, both of which include several species that range from the lower to the upper Eocene. These genera are the continental freshwater taxon *Neochelys* and the coastal taxon *Eocenochelus*, adapted to life in brackish and shallow saltwater marine environments (see Pérez-García, 2017, and references therein). Despite the relative abundance of osteological remains, only one locality from the Eocene of France has provided putative turtle eggs (Department of Bas-Rhin, Kuntz, 1981) although no microstructural analysis has been carried out to confirm this identification. Thus, no eggs or eggshell fragments of testudines have been unambiguously identified in the Eocene, despite the relative abundance of osteological remains in all continents.

Extant pleurodiran turtles are known to nest in different lentic and lotic environments within modern continental and deltaic aquatic systems, all of them being freshwater forms (see Pérez-García, 2017, and references therein). Nevertheless, the Eocene pleurodiran *Eocenochelus eremberti* is thought to have inhabited near-coastal areas (Pérez-García et al., 2021).

Extant turtles prefer sandy sediments, when available, to lay their eggs (Kuchling, 1999), and all extant marine turtles dig their nest in sandy supratidal areas (Hendrickson and Balasingam, 1966; Stancyk and Ross, 1978; Bonach et al., 2011), resorting to clay or silt substrates only when sand is scarce. Even in these cases, nesting in muddy substrates results in high mortality rates, due to the differences in humidity and temperature exchange in these nests (Mortimer, 1990; Marco et al., 2017). If sand bars are not available in their habitat, turtles (e.g., the cryptodiran *Batagur baska*) are known to travel several tens of kilometres up freshwater streams in order to find adequate nesting substrates (Pritchard, 1979; Kuchling, 1999).

The middle Eocene (Lutetian) fossil site of Castejón de Sobrarbe-41 (CS-41) is a monodominant sirenian bonebed located in the southern Pyrenees (Ainsa Basin, Huesca province, Spain). Together with the abundant sirenian remains, turtle fossils have been recovered from the site. These include a complete shell assigned to the Eocene pleurodiran turtle *Eocenochelus eremberti* (De Broin, 1977). This shell increased the previously recognized palaeobiogeographical distribution of the species (Pérez-García et al., 2021). In addition to macrofossil remains, abundant microfossils have been recovered in this fossil site. The microfossil assemblage includes chondrichthyan, osteichthyan, crocodylomorph, squamate and micromammal teeth, fish otoliths, invertebrates (gastropods and bivalves), plant remains, and an anomalous concentration of eggshell fragments.

Here we describe the first confirmed Testudines eggshells from the Eocene, from the CS-41 site. We discuss the unusually high concentration of eggshell fragments, all attributable to a single ootaxon and found in association with turtle skeletal remains, the first known concentration of several individuals of *Eocenochelus* to be identified. We undertake a precise assessment of the sedimentology of the assemblage and the surrounding environment, concluding that the eggshell assemblage of CS-41 was the result of an event that dismantled *Eocenochelus* nesting grounds located in sandy deposits within the delta mouth and deposited them in an abandoned channel in the deltaic plain.

2. Geological setting

The palaeontological site CS-41 is located in the Spanish South Pyrenean Zone in the Aínsa Basin (Fig. 1A,B). This basin represents the easternmost sector of the Jaca-Pamplona Basin, located in the transition zone with the Tremp-Graus Basin (Barnolas and Pujalte, 2004; Muñoz et al., 2013). The study site is protected, but exact location information can be shared with qualified researchers upon request.

During the middle Eocene, the South Pyrenean Zone was a narrow gulf opened to the Atlantic Ocean. The fragmentation of the previously continuous South Pyrenean Basin began in the late Ypresian with the southwards transport and the continentalization of the piggy-back Tremp-Graus Basin, dividing the South Pyrenean Basin into the Jaca-Pamplona Basin to the west and the Eastern South Pyrenean Basin to the east (Barnolas and Gil-Peña, 2001). Lutetian sedimentation in this area evolved from a deep submarine fan and slope deposits (San Vicente Formation, Lunsen, 1970) to a shallow marine shoreface environment in the middle Lutetian (Sobrarbe Formation, de Federico, 1981), followed by a continentalization of the area during the late Lutetian (Bentham and Burbank, 1996; Bentham, 1992; Escanilla Formation, Garrido Mejias, 1968). Due to the interfingering and genetic relations of these units, Dreyer et al. (1999) included the upper part of the San Vicente Formation, the Sobrarbe Formation and the lower to middle part of the Mondot Member of the Escanilla Formation in the Sobrarbe Deltaic Complex.

The materials studied in the CS-41 site correspond to the Sobrarbe Formation. This heterolithic unit is composed of slope mudstones, shoreface coarse sandstones, and gravels, marls, siltstones, and fine-grained sandstones from a marginal marine setting. The Sobrarbe Formation represents the delta front to delta plain environments within the Sobrarbe Deltaic Complex (Dreyer et al., 1999). The Sobrarbe Deltaic Complex is composed of various transgressive-regressive sequences that led to an overall regression corresponding to the top of the Sobrarbe Formation, and the expansion of continental environments above this unit (Dreyer et al., 1999). The CS-41 site is located in the upper part of the Sobrarbe Formation, in an interval characterized by marginal marine, delta plain deposits.

The Sobrarbe Deltaic Complex has been described as fluvially influenced (Dreyer et al., 1999; Ubeid, 2008). In the middle Eocene, the Aínsa Basin was located at a latitude similar to the present day (Advokaat et al., 2014; Rosenbaum et al., 2002). Nevertheless, due to the globally warm Eocene temperatures the Sobrarbe Delta was influenced by a subtropical climate, frequently affected by storm events (Hall, 1997; Ubeid, 2008).

3. Materials and Methods

This study is based on 12,088 eggshell fragments, all of them identified under the binocular microscope. Twenty specimens (MPZ 2021/55 to MPZ 2021/74) were prepared for scanning electron microscope analysis (secondary electron imaging); five were prepared as

153 petrographic thin sections (MPZ 2021/75 to MPZ 2021/79); and one (MPZ 2021/80) was
154 prepared as an ultra-polished thin section for electron backscatter analysis.

155 In addition to the already published Testudines material from CS-41 (MPZ 2019/263),
156 three additional partial plastra of *Eocenochelus* are here described for the first time (MPZ
157 2021/83, MPZ 2021/81, MPZ 2021/82). Finally, six partial plates attributed to Cryptodira indet.
158 (MPZ 2021/84 to MPZ 2021/89) are included.

159 3.1. Microfossil sampling

160 Rock from the CS-41 site was sampled during the digging of the macrovertebrate fossil
161 assemblage, both to recover fractured and small macrovertebrate bones and to gather
162 microfossil remains such as small-vertebrate, invertebrate and plant remains. The digging
163 procedure was to collect one out of every two sacks of rock refuse (12 to 22 kg) for a total of
164 300 to 400 kg of bulk dry rock per season. The digging site was divided into a grid of squares 1
165 m by 1 m, and each sample was labelled with both the grid number and the date. Exceptions to
166 this procedure included samples collected around exceptional specimens, such as the skulls and
167 hipbones of sirenians, and articulated remains, where all the refuse was collected, and its exact
168 coordinates recorded. Discarded refuse was saved in two dump piles close to the digging site,
169 where it could be retrieved if needed for future analysis.

Commented [rg1]: ¿ok así?
Es decir, cada casilla = 1 x 1 m

170 The samples were left to dry in the sacks for at least one week and then soaked in water
171 with a small amount of peroxide (less than 5%). Afterwards, the samples were screen-washed
172 with sieves of descending mesh size (2, 1 and 0.5 mm). The resulting concentrates were then
173 picked through under a binocular lens. Approximately 600 kg of rock have been processed over
174 the last 10 years. The CS-41 site is very rich in microfossil remains, especially teeth, fish otoliths
175 and eggshells, although not all the bonebed is equally rich (see sedimentological analysis). In
176 this study we selected three samples at random corresponding to Facies 3, the richest of the
177 three identified facies on the site. The approximate location of the samples analysed is provided
178 in Supplementary Figure 1.

179 In the present work, in order to assess the relative abundance of each fossil type in CS-
180 41, three samples of rock were selected, washed with the standard procedure, and carefully
181 picked through, counting all the remains. The outcome of the picking procedure is detailed in
182 the Results section and in Table 1.

3.2. Sedimentological analysis

The general stratigraphic and sedimentological framework of CS-41 was assessed based on the stratigraphic section in Fig. 1C, located in the upper part of the Sobrarbe Formation. The section includes a ~50 m continuous succession below the palaeontological site itself, in order correctly to define the sedimentary environment where the entire succession was deposited. This section was then correlated with the sedimentary facies model proposed by Dreyer et al. (1999) for the Sobrarbe Deltaic Complex.

Taphonomic observations are based on a detailed mapping of the site (see Supplementary Figure 1) and notes acquired during the excavation of the site. A preliminary report on the taphonomy of CS-41 is provided in this work, although the complete biostratinomy of the locality is a work in progress (see Diaz-Berenguer, 2020, for a preliminary study).

In addition, two detailed stratigraphic profiles of the C-41 site were produced to provide further sedimentological data on the site formation. These sections were elaborated during the 2020 digging season, in the coordinates X:210, y:700; and X:0 to 200, y:900. Samples of rock were collected every 5 cm of the profile in order to analyse trends in the granulometry of the site.

Grain-size analyses were undertaken at the Instituto de Carboquímica-CSIC (Zaragoza). The particle-size distribution of each sample was measured using a Beckman Coulter LS 13 320 laser diffraction particle size analyser. The data were plotted on a size-frequency curve, which provides sufficient statistical and geometric information.

3.3. Eggshell analysis

The eggshell fragments were sorted under an Olympus SZ40 binocular microscope. Two groups of eggshells were recognized: those with compactituberculate ornamentation and those with apparently flat outer surfaces (see description below). Selected fragments were embedded in epoxy resin and prepared in 30-µm thin sections in radial view. The thin sections were examined and photographed with an Olympus AX-70 petrographic microscope equipped with an Olympus E-330 digital camera, housed in the “Servicio de Microscopía Óptica e Imagen” of the University of Zaragoza. Over a hundred fragments were cleaned using an ultrasonic bath for 15 minutes and mounted using both fresh-cut surfaces and non-cut edges for scanning electron microscopy (SEM), gold-coated, and then examined in a JEOL 6400 SEM housed in the “Servicio de Microscopía Electrónica de Materiales” of the University of Zaragoza.

A single thin section was chosen for electron backscatter diffraction after examination under the petrographic microscope. This sample was carefully polished with diamond, alumina and colloidal silica to achieve a flat acquisition surface. The sample was then carbon-coated and examined with a Carl Zeiss MERLIN™ FE-SEM, equipped with an Oxford EDS INCA 350 detector and an EBSD detector. Kikuchi lines were captured and indexed using AZtec software (Oxford Instruments) with a step size of 1.50 µm. Wild spikes were removed, and zero solutions were extrapolated using Channel5, from up to six neighbours. The analysis setting was as follows: accelerating voltage 15.0 kV, working distance 20.0 mm, and tilting of the specimen 70 degrees. Maps were constructed to present the data, including all-Euler misorientation maps showing the relative misorientation between domains, inverse pole figure (IPF) maps showing the orientation of the c-axis of the carbonate crystals, and grain boundary maps (5°–10°, 10°–20° and > 20° degrees of disorientation), following Choi et al. (2018).

All materials were collected under the local regulations (Dirección General de Patrimonio Cultural, Gobierno de Aragón). The fossils are housed in the Museo de Ciencias Naturales de la Universidad de Zaragoza (MPZ, Canudo et al., 2018).

4. Results

4.1. Sedimentology and sedimentary environment

Description

The Castejón de Sobrarbe stratigraphic section is divided into three intervals according to the predominant facies (Fig. 1C). Over a non-accessible three-metre bed of marls, coarse-grained sandstones, interbedded with blue marls, characterize the lower interval (metres 3 to 12). These sandstone bodies typically exhibit trough cross-stratification, although at the base of the interval a single bed of sigmoidal cross-stratification is observed. Bioturbation is absent at the base of this interval, and common in the upper part (vertical burrows). Body fossils are restricted to one interval with complete oyster shells in a poorly sorted microconglomerate.

The middle interval (metres 12 to 21) is composed of bluish-grey marls and coarse-grained cross-stratified sandstones and limes. The bluish-grey marls, partially covered, dominate the lower part. These marls pass upwards to bioturbated siltstones, which exhibit well-developed lamination at the top. The upper part is composed of coarse-grained cross-stratified sandstones. This sandstone body is laterally discontinuous, and a lateral thinning is observed, from three to one metre. Bioturbation is ubiquitous, consisting of vertical, horizontal, and U-

shaped burrows. At the base and the top of this sandstone body, abundant macrofossils are observed, including echinoids, oysters and other bivalve remains. Scarce isolated vertebrate remains can be found at the top.

The upper interval (metres 21 to 49) is characterized by fine-grained lithologies, with a dominance of silty marls interbedded with fine and medium-coarse-grained sandstones. The brown silty marls range from partially laminated and structureless to mottled with occasional root bioturbation. Among the coarser lithologies, two types are observed: medium-grained sandstones and very fine sandstones to siltstones. The medium to coarse-grained sandstones are arranged in metre-thick beds and exhibit cross-stratification and wavy bedding, although these structures are locally obliterated by bioturbation. The thinner lithologies correspond to very fine-grained sandstone to siltstones, with parallel lamination and occasional cross- or ripple lamination. They occur as sandstone bodies of less than a metre scale, with low bioturbation. In the upper part of the interval, desiccation cracks can be observed at the top of these fine-grained sandstone beds.

The CS-41 site is located at the top of the upper interval (Fig. 1C, Fig. 2). The fossil assemblage is restricted to an accumulation one metre wide and over six metres long, with an irregular pseudo-canaliform base (Supplementary information S1). The fossils are found in an eighty-centimetre-thick interval of brown silts. As a result of ongoing erosion and edaphic processes, together with the excavation of the site, only the bottom fifty centimetres of the bone-bearing sequence are currently preserved and have been sampled for this study. The proximity of the fossiliferous bed to the surface, and the location of the fossil site in the middle of a forest have resulted in intense modification of the outcrop due to the action of vegetation, hampering the observation of some of the taphonomic and sedimentological features.

Three different facies can be differentiated in the profile of the CS-41 site (Figure 2). Facies 1 is present below the bonebed and consists of an orange-brown, poorly sorted medium silt with a unimodal, symmetrical, mesokurtic grain-size distribution. This facies has planar cross-bedding lamination, and invertebrate ichnofossils. Both macro- and microfossils of vertebrates are extremely rare in this facies. Facies 2 is a 13-centimetre bed of brown-greyish, very poorly sorted fine sandy coarse silt, with a polymodal, symmetrical, mesokurtic grain-size distribution, with planar cross-lamination and nodulization. The bed has a gentle canaliform base and irregular top. Macrofossil remains are very scarce, with fewer than three bones per square metre. Microfossil remains are also scarce. Facies 3 comprises the bonebed, and it is a 40-to-60-centimetre bed of brown, poorly sorted silts, with a unimodal, symmetrical, mesokurtic grain-

size distribution, with planar lamination disrupted by the bone accumulation, sandy rip-up clasts from the underlying bed, and frequent organic matter drapes. Macrofossils are very abundant, and include wood fragments, *Teredolites*, and mainly sirenian and turtle bones. The bones are complete, although articulated specimens are extremely rare, except for turtle shells. Noteworthy is that no embryonic remains of turtles have been identified in either the macrofossil or the microfossil association. Laterally, the bone-bearing bed passes to poorly laminated, brownish silty marls with scarce fossils. Finally, the top 10 centimetres of the fossiliferous bed are heavily disrupted by weathering and the evolution of the present-day edaphic level overlying the palaeontological site.

Interpretation

The stratigraphic succession observed in the Castejón de Sobrarbe section is characteristic of a deltaic environment. The fining-upwards sequence observed in this section suggests the transition from a high-energy environment in a delta front environment to a low-energy setting in the delta plain.

The lower interval corresponds to a mouth-bar complex in a delta front environment. The abundance of coarse-grained deposits indicates deposition in a high-energy environment. The sandstone body comprising the lower interval can be followed several hundred metres on the field. The occurrence of these sandstones interbedded with grey marls, the presence of marine fossils, and the sequence itself (the structureless sandstones with marine fossils located underneath the section described) justify the definition of this interval as a mouth-bar complex (Dreyer et al., 1999; Ubeid, 2008).

The middle interval represents the transition from the delta front to a quieter environment in the delta plain. The bluish-grey marls in the lower part of this interval represent an interdistributary bay. The dark colour of these marls evidences a poorly drained environment in a subtidal to intertidal environment. The sandstone body above represents a distributary channel. This interpretation is based on the shape of this body (thinning laterally from three metres to only one metre, most probably discontinuously), and the presence of marine fossils at the base and on top of these sandstones.

The upper interval represents a delta plain facies association. The predominant brown silty marls were deposited in a moderately drained overbank environment. The medium-grained sandstones are interpreted as intertidal distributary channels, due to the presence of tidal sedimentary structures (wavy lamination) and bioclasts. The fine-grained, laminated sandstones to siltstones, on the other hand, are interpreted as crevasse-splay deposits. A similar facies

association has been described by Dreyer et al. (1999) and Ubeid (2008) across several other sections of the Sobrarbe Deltaic Complex. The CS-41 fossil site was deposited in the context of this delta plain facies.

The fossiliferous bed overlies a medium-grainedsilt bed with continuous lateral extension. Overlying this bed, an erosive, canaliform, fining-upwards deposit contains the bonebed. This bed was formed as a single-event deposit, eroding the underlying bed, and exhuming the fossils and sediments as the deposit was formed. Its canaliform base and reduced lateral extension, together with the spatial distribution of the vertebrate macrofossils recovered, points towards the infill of an abandoned channel during an energetic event.

4.2. Systematic Palaeontology

Oofamily Testudoolithidae Hirsch, 1996

Oogenus and oospecies indet.

Figures 3 and 4

Description

Eggshell fragments are among the most common microfossils in the assemblage from CS-41 (see Table 1). The fragments are small to very small, most of them less than 2 mm in their longer axis, and they are caramel brown in colour. The fragment preservation is highly variable, ranging from pristine eggshells (e.g., Fig. 3A, D) to fragments with clear signs of abrasion (e.g., Fig. 3E). The size and shape of the eggs cannot be evaluated due to the small size and fragmentary nature of the specimens.

The CS-41 eggshells are thin (ranging from 210 µm to 395 µm; 283 µm mean thickness, SD=38 µm; n=66) and single-layered, formed by strongly interlocking, barrel-shaped, domed shell units, with a height-to-width ratio of 1.6/1 to 2.4/1. Secondary electron images of radial sections show different degrees of preservation of the original aragonite radial ultrastructure. Some eggshell fragments, such as MPZ 2021/56 (Fig. 3A), show phantoms of the acicular crystals radiating from the cratered bases of the shell units to the external surface, whereas in most fragments, such as MPZ 2021/55 and MPZ 2021/58 (Fig. 3B, C), the radial ultrastructure has been completely obliterated, and calcite pseudo-rhombohedra of up to 50 µm have replaced the original aragonite. Large (5–15 µm) pits, resembling vesicles, are present throughout the eggshell section, but are variable in size and distribution among the different eggshell fragments,

suggesting that they are secondary structures caused by the change in volume of the carbonate crystals during recrystallization. Alternatively, acid etching may have affected some of the fragments, most likely related to present-day edaphic processes. The pore channels are straight and funnel-shaped, with a minimum width of 35 µm in the middle section of the pore, and up to 80 µm at the pore opening at the external surface.

The external surface of the eggshell displays compactituberculate ornamentation, as a result of the barrel-shaped, domed shell units. Most nodes are subcircular, but oval nodes are also present. The nodes appear clustered in groups of two to over 10, delimited by the pore openings situated in the spaces between the shell units (white square in Fig. 3D). These clusters of nodes are the expression in the external surface of the interlocking shell units and seem to occur randomly throughout the eggshell. As a result, small shallow valleys appear between non-interlocking shell units, giving the external surface a wormy aspect. Pore openings occur either isolated or within these valleys, suggesting that their distribution is independent of the shell unit configuration. Some eggshell fragments exhibit relatively smooth outer surfaces, where the nodes are less marked (Fig. 3B). This is the result of two independent taphonomic alterations: the smoothening of the eggshell by abrasion (Fig. 3B) or the presence of an outer layer of diagenetic calcite masking the ornamentation (Fig. 4D).

In the inner surface, the bases of the shell units are tightly abutted, leaving only minor interstices between shell units other than the pore openings. All the inner surfaces examined present cratered bases, with relatively large exposed organic core sites (=primary spherites 65 µm in diameter, SD=18 µm, N=20). This has been interpreted as related with hatched eggs but could also be the result of abrasion during transport (Bravo et al., 2003; Oser and Jackson, 2014). The tight packing of the shell units is evidenced by the abundance of suboval, appressed shell units, which have been compressed between their neighbours (Fig. 3E, G). Some of the shell units are so tightly interlocked that the boundaries between adjacent units are highly reduced, resembling “twin” primary spherites (Fig. 3H). Nevertheless, a double boundary of crystals is always present, even in the most tightly packed craters.

In thin section, the eggshells also show the typical barrel shape of the shell units. A fine radial texture can be observed in parallel-polarized light, showing the relics of the original aragonite radial ultrastructure. The funnel shape of the pore openings can be observed in Fig. 4A. Some shell units preserve the organic cores whereas most of them have cratered bases. In cross-polarized light the recrystallized condition of the eggshells is highlighted. Large sub-euhedral calcite crystals with a blocky extinction pattern have completely replaced the original

aragonite radial crystals, with some shell units being formed by as many as two large crystals, and some crystals crossing shell unit boundaries (Fig. 4C). The large size of the crystals, together with the presence of acicular crystal phantoms, suggests an extremely slow recrystallization process. Nevertheless, other eggshell fragments show smaller calcite crystals obliterating the eggshell structure (Fig. 4B), suggesting that the speed of the recrystallization was not homogeneous in the assemblage. Growth lines are absent throughout the shell units.

Electron Backscattered Diffraction (EBSD)

Phase maps elaborated for calcite (-3m) and aragonite (Pmcn) show that only small relics of the original composition are preserved (red areas in Fig. 4E). The largest of these areas has only 10 pixels (7.5 x 4.5 microns) and is close to a pit in the section surface, so it cannot be ruled out that these areas are indexing artefacts. Relics of aragonite in fossil ghosts have been previously detected with EBSD (Balthasar et al., 2011), but the proportion of preserved aragonite was much more significant than in our study, suggesting that the original eggshell composition has been completely lost in the Castejón de Sobrarbe-41 eggshells. This is supported by inverse pole figure orientation maps (Fig. 4F), which show a strong realignment of the c axes of the calcite grains at an angle of 60° with the dominant eggshell growth direction. Most of the eggshell shows large calcite grains (up to 120 µm) with high-angle (>20°) misorientation boundaries between neighbours (Fig 3G). All the above is coherent with the single, slow recrystallization of the original metastable aragonite composition to a more stable low-magnesium calcite composition. Variations in the degree of preservation between different eggshell fragments are due to the irregularity of the crystallization process, can be observed within a single eggshell fragment, and cannot be related to different origins of the eggshells.

Comparison

All eggshell fragments found in CS-41 are attributed to a single ootaxon, as the minimal differences observed in eggshell thickness and ornamentation can be attributed to differences in preservation. All of them exhibit the same barrel-shaped units and funnel-shaped pore channels.

The CS-41 eggshells can be attributed to Testudinata on the basis of their subcylindrical shell units with a radial ultrastructure, originally composed of aragonite, now fully replaced by more stable calcite. A similar taphonomic process has been described in turtle eggshells from the Upper Cretaceous of Madagascar (Lawver et al., 2015). The spherurigidis morphotype and the tightly abutting shell units are diagnostic of the oofamily Testudoolithidae. Four oogenera have been described within this oofamily: *Testudoolithus* Hirsch, 1996; *Chelonoolithus* Kohring,

1998; *Emydoolithus* Wang et al., 2014; and *Haininchelys* Schleich et al., 1988. The diagnosis of all four oogenera is problematic, as there is a high degree of overlap in the characters used (see Lawver and Jackson, 2014, for updated details on the diagnoses). The CS-41 eggshells are thicker than those of *Chelonoolithus* (Kohring, 1998), which also show relatively wide shell units, with an aspect ratio of 1:1. They are thicker than those of *Emydoolithus* and of most oospecies and specimens referred to the oogenus *Testudoolithus*, but fall within the diagnosis of the type oospecies *Testudoolithus rigidus* from the Miocene of the USA, with a shell unit height-to-width ratio of about 2:1, an eggshell thickness of 0.22 to 0.24 mm, and spheroidal eggs of 42 mm by 47 mm (Hirsch, 1996). Nevertheless, they differ in the funnel-shaped pore openings and compactituberculate outer surface ornamentation seen in the Eocene eggshells. *Testudoolithus zelenitskyae*, from the Late Cretaceous of North America (Zelenitsky et al., 2018, Lawver and Jackson, 2017), shares with the CS-41 eggshells the domed shell units and compactituberculate ornamentation but can be easily differentiated in being twice as thick (660–760 µm in non-pathological eggshells) and having shell units with a greater height-to-width ratio (3.15:1 to 5.5:1).

The current whereabouts of the type material of *Haininchelys curiosa* is unknown. Thus, the only comparisons currently possible are based on the photographed materials published by Schleich et al. (1988). The CS-41 eggshells are indeed comparable with *Haininchelys*, sharing a similar eggshell thickness and shell unit h/w ratio. Despite not being included in the original diagnosis of *Haininchelys curiosa*, moreover, CS-41 shares with *Haininchelys* the funnel-shaped pores and compactituberculate ornamentation. Differences observed include the relatively large primary spherites of the Spanish eggshells (20 to 40 µm versus 60 µm), although it must be noted that this measure was acquired at the cratered bases of the mammillae and may be exaggerated by both biological and geological erosion. Nevertheless, we refrain from ascribing the Testudoolithidae eggshells from CS-41 to the oogenus *Haininchelys* for two main reasons: 1) the unavailability of the type materials of *Haininchelys*, which precludes direct comparison of the specimens; and 2) the advanced recrystallization observed in the Spanish specimens, which, while allowing the preservation of the most diagnostic characters, prevents detailed description of the eggshell ultrastructure.

Schleich et al. (1988) compared *Haininchelys* with eggs of the extant pleurodiran turtle *Emydura subglobosa* (Krefft, 1876), which shares the funnel-shaped pore openings and the nodose ornamentation of the outer surface, while also presenting other characters such as multiple twinned primary spherites. They thus suggested that *Haininchelys curiosa* was laid by pleurodiran turtles. Winkler (2006) studied the phylogenetic distribution of the eggshell

443 characters in pleurodires and demonstrated that the turtle egg was highly homoplasic, with
444 characters such as egg shape, surface ornamentation and shell unit shape highly variable among
445 different clades. Winkler (2006) also reported that the shape and distribution of the pore
446 openings, together with the interstice dimensions between shell units, were the only characters
447 that recovered real clades. Thus, outer surface ornamentation is observed both in cryptodiran
448 (e.g., *Chelydra serpentina*; Packard, 1980, fig. 4; *Sternotherus minor*; Packard et al., 1984, fig. 1B;
449 *Apalone* spp. Lawver et al., 2017, fig. 5) and pleurodiran turtles (e.g., *Erymnochelys*
450 *madagascariensis*; Winkler, 2006, fig. 1B; *Emydura subglobosa*, Lawver, 2017). *Apalone*
451 eggshells can be easily differentiated from CS-41 eggshells in being much thinner (ranging
452 between 88 µm and 192 µm in the different species), having units that are wider than tall or
453 only slightly taller than wide (h/w ratio 0.9/1 to 1.4/1), presenting growth lines, and having
454 irregular accessory aragonite crystals filling the spaces between shell units, a condition not
455 observed in the Testudoolithidae indet. from CS-41. Finally, most cryptodiran turtles show
456 straight pore channels without a variable section (Winkler, 2006). The pleurodirans
457 *Erymnochelys madagascariensis* and *Emydura subglobosa* are the only extant turtles for which
458 funnel-shaped pore channels have been described.

459 The CS-41 eggshells resemble those of *Emydura subglobosa*, which show the same
460 compactituberculate ornamentation and domed shell units. Nevertheless, *Emydura* eggshells do
461 not show any interlocking shell units but have spaces between adjacent units; they have curved
462 growth lines throughout the shell unit, and are significantly thinner (190 µm; Lawver, 2017). In
463 addition, the pore channels of the CS-41 eggshells are twice as wide as those of *Emydura* (16–
464 51 µm; Lawver 2017). Similarly, the CS-41 eggshells are similar to the eggshells of *Erymnochelys*.
465 They share the compactituberculate ornamentation and funnel-shaped pores. Furthermore,
466 Winkler (2006) reports interlocking shell units for *Erymnochelys madagascariensis* eggshells,
467 although this character is reported as variable (Winkler, 2006, fig. 2). The eggshells are thinner
468 than those of CS-41 (210 um according to Winkler, 2996, fig. 1B, with units as wide as tall, or
469 taller than wide). The presence or absence of the growth lines has not been reported.

470 Phylogenetic studies focusing on turtle eggshell structure show that turtle eggshell is
471 highly homoplasic, and no traits can be regarded as synapomorphies of Pleurodira or Cryptodira.
472 Nevertheless, Testudoolithidae indet. of CS-41 bear the greatest resemblance to the eggshells
473 of two pleurodiran taxa, so the hypothesis that they were laid by turtles belonging to this lineage
474 cannot be ruled out.

4.3. Biostratinomy of the CS-41 vertebrate fossil assemblage

The CS-41 macrofossil assemblage is a monodominant sirenian bonebed. A total of 703 macrovertebrate fossils have been recovered, the most abundant belonging to the quadrupedal stem pan-sirenian *Sobrarbesiren cardieli* (Díaz-Berenguer et al., 2018, 2020), including cranial and postcranial bones of at least eight individuals. This is followed by turtles and scarce crocodylomorph teeth and bones (Díaz-Berenguer et al., 2018). The fossils are complete and well preserved, although some are fractured due to lithostatic compression and recent plant bioturbation. The bone remains are poorly sorted, and disarticulated, with the exception of one almost complete and several partial turtle shells belonging to the pleurodiran *Eocenochelus*. Furthermore, the physicochemical weathering is insignificant, suggesting a short period of subaerial or subaquatic exposure before burial (Behrensmeyer, 1975; Boessenecker et al., 2014, and references within). In contrast, cryptodiran turtle remains are scarce and are disarticulated, with only six isolated plates identified as belonging to cryptodiran turtles from the total of 703 specimens recovered (Supplementary information S1 and S2; see Discussion).

The study of the spatial bone distribution (Supplementary information S1) shows a concentration in an area one metre wide by at least six metres long, with a north-northeast to south-southwest direction, bending gently towards the east. Furthermore, most of the bones with an elongated axis (mainly sirenian ribs) that are not contacting other bones are oriented with the long axis in a N-S or E-W direction. Indeterminate bivalve shells, *Teredolites* fragments, and wood fragments are also present in the assemblage.

The CS-41 microfossil assemblage is composed of disarticulated remains of osteichthyans, chondrichthyans, squamates, eusuchian crocodylomorphs, micromammals, vertebrate eggshell fragments, gastropods, bivalves, and plant remains (Díaz-Berenguer et al., 2018). The three rock samples analysed for microfossil samples are dominated by eggshell fragments (Table 1). The richest subsample (21 kg) provided a total of 10,841 microfossil remains (Fig. 1D, Table 2). Of these, 6,777 were eggshell fragments, the equivalent of 322.7 eggshell fragments per kilogram of processed rock. Eggshells represent 63% of the total microfossils recovered in the sample (Fig. 1C), followed by 35% corresponding to other vertebrate remains, including complete and fragmented bones and teeth. Invertebrates (gastropods, bivalves and indeterminate mollusc fragments), foraminifera and plant remains (wood fragments) represent only 2% of the total. With respect to vertebrate remains only, eggshells represent 64% of the elements found in the sample, whereas bone elements represent 36% of the sample, and enamel elements (teeth and scales) represent less than 1%. The other two subsamples are less rich in microfossil content but are also dominated by eggshell fragments (CS41-C16/17, 68%,

1,596 eggshell fragments in 12 kg of unprocessed rock; CS41-C19/20, 81%, 3,961 eggshell fragments in 14 kg of sediment).

Most of the microfossils are well preserved, and most of the observed breakage can be attributed to the extraction process. Nevertheless, the relatively low abundance of enamel elements, more resistant to transport and abrasion, suggests that the fossils have not undergone long-distance transportation (Fig. 1D).

5. Discussion

5.1. The Eocene record of turtle eggshells

The eggshells here described represent the first report of Testudinata eggshells from the Eocene anywhere in the world. This is surprising, as turtles are common components of fossil assemblages at least since the Late Jurassic, the clade being known since the Late Triassic (Li et al., 2018), and turtle hard eggshells are known from almost every period from the Lower Jurassic to the present (Buckman, 1860; see Lawver and Jackson, 2014, for a detailed revision of the fossil record of turtle reproduction). In general, few instances of Eocene fossil eggshells are known, including crocodylomorph and avian eggs (Hirsch, 1985; Jackson et al., 2013, and references within).

Most probably, the scarcity of the record is due to a sampling bias. It is true that eggs, clutches, and nests are rare fossils for most of the Mesozoic, with a few exceptions probably related to large-scale colonial nesting (Chiappe et al., 1998; Vila et al., 2010). Even so, eggshell fragments can be found in most continental environments when systematic screen-washing is undertaken, even in areas or facies where eggs are unknown (Buscalioni et al., 2008; Gasca et al., 2012; Núñez-Lahuerta et al., 2019). Further systematic sampling of Eocene outcrops is required before ascribing biological or ecological significance to the absence of oological remains in this period.

5.2. Taxonomic affinities of the CS-41 eggshells

All the eggshells recovered in CS-41 can be referred to a single ootaxon in the oofamily Testudoolithidae. This does not imply a single egg-laying taxon, as eggshell characteristics are both highly conservative within the family level (Mikhailov et al., 1996) and highly homoplasic (Winkler, 2006), but the low variance of the sample suggests that a single species of egg-layer is the most parsimonious hypothesis. In the absence of embryos or gravid specimens, it is difficult

to be confident in attributing an ootaxon to an egg-layer, although, following Mikhailov et al. (1996), inferences with different degrees of confidence can be based on the eggshell morphology and the fossil record of the Sobrarbe Formation.

The ultrastructure and the original aragonitic composition inferred for the eggshell allow the taxonomic assignment to be narrowed down to Testudinata, and the morphology of the shell units, the outer surface ornamentation, and the pore channels are more compatible with a member of Pleurodira than of Cryptodira.

In the Sobrarbe Formation, five turtle taxa have been reported: three cryptodires (an indeterminate testudinid, a trionychid and a carettochelyid; Pérez-García et al., 2013) and two pleurodires (*Neochelys* cf. *salmanticensis* and *Eocenochelus eremberti*; Pérez-García et al., 2013, 2021). To date, a single turtle fossil from the CS-41 site has been studied. This corresponds to an almost complete shell, representing one of the few relatively complete shells of *Eocenochelus* so far known (Pérez-García et al., 2021). It was attributed to the type species, *Eocenochelus eremberti*, previously only known in the Franco-Belgian Basin (Pérez-García and Smith, 2017). The recent preparation and study of the other turtle remains found in this site have revealed that the turtle assemblage of CS-41 is dominated by a single taxon, *Eocenochelus eremberti*. In fact, this is the only palaeontological region where more than a single specimen of *Eocenochelus* can currently be identified: so far, all other identifications of this taxon in European lower, middle, and upper Eocene levels have corresponded to isolated findings. Thus, although findings of accumulations of freshwater turtle remains are relatively common (for example, those of the European Eocene pleurodire *Neochelys*), remains of coastal forms are generally much scarcer in the fossil record (Pérez-García and Smith, 2017). At least four individuals belonging to *Eocenochelus eremberti* are recognized here as present in CS-41 from the study of articulated and partial shells (see Fig. 5). These can be attributed to Pleurodira on the basis, among other characters, of the presence of a pair of lateral mesoplastra, scars from sutured contacts of the pelvis with the shell, and the presence of a single intergular scute (De Broin, 1980; Gaffney et al., 2006). They are recognized as members of Erymnochelyini, differing from the other European podocnemidids (i.e., *Neochelys*), by characters such as their sub-rounded anterior plastral lobe and especially the medial contact of the gular scutes, which represents a synapomorphy of this lineage (Pérez-García et al., 2021). The presence of the posterior plastral lobe that is narrower than the anterior (Fig. 5C-D); the absence of well-developed gular protrusions (Fig. 5B-C); the relatively long intergular, reaching the anterior margin of the entoplastron or overlying the most anterior region of this plate (Fig. 5B-C); and the very short dorsal expansion of the plastral scutes, allow the new remains studied here to be attributed to

573 the genus *Eocenochelus*, as was the case with the complete shell MPZ 2019/263 (Fig. 5A) (Pérez-
574 García et al., 2021). Some of these new remains are as large as those known for some specimens
575 of *Eocenochelus eremberti*, this species being larger than the other representatives of this genus
576 so far identified. In addition, they show a character exclusive to *Eocenochelus eremberti* (the
577 anterior margin of the intergular narrower than that of each gular; Fig. 5 B-C; Pérez-García and
578 Smith, 2017).

579 In addition to these articulated specimens, numerous isolated plates probably
580 attributable to this species, as well as well-preserved appendicular elements that are also
581 compatible with it, demonstrate the abundance of this form and its good preservation. By
582 contrast, only scarce indeterminate plates attributable to an ornamented member of Cryptodira
583 (either a trionychid or a carettochelyid), disarticulated and fragmented in the biostratinomic
584 stage, have been found (Supplementary information S2). The accumulation of abundant well-
585 preserved remains (without significant weathering and without abrasion) of the coastal turtle
586 *Eocenochelus* thus implies that its remains did not undergo significant transport, and that they
587 were buried relatively quickly, in contrast to the cryptodirans.

588 Lacking *in ovo* embryos or gravid females, it is impossible to ascertain definitively the
589 identity of the egg-laying species of the CS-41 eggshells. Proposed spatial relationships between
590 osteological remains and eggs have been proven wrong in the past (e.g., Jackson et al., 2018).
591 Nevertheless, two independent lines of evidence strongly support the relation between the
592 osteological and oological fossil remains of CS-41: first, the unusual concentration of eggshell
593 fragments, all of them belonging to the same turtle-related ootaxon; and second, the presence
594 of abundant articulated pleurodiran remains, especially in contrast with the scarce and
595 disarticulated cryptodiran remains. Thus, the information currently available leads us tentatively
596 to identify the CS-41 eggshells as belonging to a pleurodiran turtle.

597 As mentioned above, the eggshell structure of the turtle eggshells from CS-41 bears a
598 greater resemblance to the eggshell of *Erymnochelys madagascariensis* and *Emydura*
599 *subglobosa* than to that of any other extinct or extant taxon described so far. *Emydura*
600 *subglobosa* belongs to Chelidae, a clade of Pleurodira which diverged from Pelomedusoides in
601 the Early Cretaceous and has a Gondwanan distribution (Holley et al., 2020). However,
602 *Erymnochelys* is a representative of Pelomedusoides closely related with *Eocenochelus*
603 *eremberti*, being the only extant representative of the clade to which they belong (i.e.,
604 Erymnochelyini: Pérez-García et al., 2021). Thus, the attribution of the CS-41 eggshells to the
605 genus *Eocenochelus* is the most parsimonious scenario.

5.3. Genesis of the eggshell accumulation in CS-41

Underlying the CS-41 bonebed, there is a poorly sorted, bimodal sediment, here interpreted as a low-angle crevasse-splay deposit formed on the deltaic plain. The CS-41 fossil site is interpreted as the infilling of an abandoned distributary channel, excavated on top of this crevasse-splay deposit, abandoned, and subsequently filled during a single energetic episode, where all the remains dispersed over the delta plain were trapped (Fig. 6). Such an environment receives sediment inputs from supratidal, intertidal, and subtidal sources, as well as continental fluvial inputs. The fossil assemblage reflects these mixed inputs, including parautochthonous subtidal to intertidal elements (sirenians, *Eocenochelus* shells), parautochthonous supratidal remains (i.e., eggshell fragments) and allochthonous continental elements (i.e., isolated cryptodiran plates).

With respect to the sirenian and turtle bones, the generalized disarticulation of bone elements suggests that the carcasses were skeletonized before final deposition, but the lack of signs of subaerial or subaquatic exposure suggests a rapid burial, skeletonization, exhumation and resedimentation process. In addition, the presence of most of the skeletal elements, without evidence of differential preservation, points towards an autochthonous to parautochthonous demic assemblage.

Of the microscopic fossil remains, turtle eggshells are the most abundant element recovered, with 322.7 eggshells per kilogram of sediment in the richest sample. This greatly surpasses the number of eggshell fragments recovered per kilogram of sediment in other similarly sampled localities formed by the attrition or active transport and accumulation of eggshells (see Table 2). This unusual accumulation can be explained either by a biological or physical process that favours the accumulation of eggshell fragments, or by the site's proximity to the source area of the fragments, namely a turtle nesting ground. The absence of complete eggs or large eggshells, and the depositional environment of the CS-41 fossil site are not congruent with a nesting ground. Furthermore, the degree of abrasion present in eggshell fragments has been used to identify transported eggshells (Oser and Jackson, 2014). The eggshells from the CS-41 fossil site are a mixture of unabraded (Fig. 3A, D) and abraded eggshells (Fig. 3B, E), although most fragments preserve a quadrangular morphology. This preservation suggests a certain degree of transport, although the lack of well-rounded eggshell fragments suggests that this transport was not prolonged in time. Variations in preservation may point towards multiple origins for the turtle eggshells (Oser & Jackson, 2014), although the large quantity of fragments and the lack of evidence of a sedimentological or biological accumulation agent (e.g., the lack of grain sorting or predation marks) suggest that the distance from the

source area was limited in all cases. Moreover, the lack of evidence of bioerosion in the eggshell fragments further narrows down the time span during which the eggshells remained submerged (Hayward et al., 2011), thus suggesting that there was only a short time between exhumation and re-sedimentation. The unusual abundance of eggshell fragments suggests that the assemblage was formed by the washing up of a turtle nesting ground in the proximity of the assemblage.

Turtles prefer sandy sediments for nest building (Kuchling, 1999). Muddy deposits dominate the littoral area of the Sobrarbe Deltaic Complex, as evidenced by the large amount of marls and siltites in the CS-41 section. Sandy substrates were available in the area around the CS-41 site, such as sand bars within the distributary channels along the deltaic plain (Fig. 6). The great abundance of eggshell fragments suggests that this area was used as a recurrent nesting ground, where multiple females laid their eggs. Buried hatched turtle nests do not produce surface accumulations of eggshell fragments (Jackson et al., 2015), suggesting that the clutches were exhumed by an erosive event, most probably associated with a storm, resulting in the breakage of eggs. Different nests scattered along the deltaic plain will have undergone different degrees of transport, thus explaining the different degrees of abrasion observed in the fragments. This storm event also collected animal and plant remains, including a high number of sirenian bones, together with the first known accumulation of the coastal turtle *Eocenochelus eremberti*, washing over the deltaic plain and accumulating the bioclasts in a small tributary channel within the proximity (a few hundred metres) of the source area, in turn resulting in the CS-41 assemblage. Thus, both the eggshell fragments and the skeletal remains can be considered parautochthonous and demic entities.

6. Conclusions

CS-41 has provided the first documented population of the coastal pleurodiran *Eocenochelus eremberti*, comprising at least four individuals. It is also rich in vertebrate microfossils, the most common elements in the assemblage being Testudoolithidae eggshells, with over 300 fragments per kilogram of rock. The histo- and ultrastructure of the eggshells from CS-41 is compatible with a pleurodiran affinity, being very similar to those of the extant Malagasy turtle *Erymnochelys madagascariensis*, which is the only representative of Erymnochelyini that is part of current biodiversity. Therefore, these Testudoolithidae eggshells are tentatively interpreted as corresponding to *Eocenochelus eremberti*, pending confirmation by the discovery of gravid females and/or *in ovo* embryos.

The CS-41 site is interpreted as the infilling of a tributary channel in the deltaic plain. The large accumulation of eggshell fragments is here recognized as a parautochthonous assemblage, resulting from the exhumation and subsequent re-sedimentation of an *Eocenochelus* nesting ground, most probably located in the sandy bars present at the mouth of the Sobrarbe Deltaic Complex.

Eocenochelus inhabited shallow warm seas and dispersed along the coastlines. Despite preferring saltwater ecosystems, it was able to make short incursions into inland environments in search of the sandy substrates required for nest building.

Acknowledgements

The authors would like to acknowledge the use of the *Servicio General de Apoyo a la Investigación*-SAI of the University of Zaragoza and to the Instituto de Carboquímica-CSIC (Zaragoza). Rupert Glasgow edited the English. Financial support was provided by the Instituto de Estudios Altoaragoneses, (XXXII Concurso de ayudas para proyectos de investigación), the Fundação para a Ciéncia e a Tecnología (PTDC/CTA-PAL/31656/2017 and UID/GEO/04035/2019), the Ministerio de Economía y Competitividad (CGL2013-47521-P and CGL2017-85038-P, MINECO/ERDF, EU), the Ministerio de Ciencia, Innovación y Universidades (IJCI-2016-30427), the Research Groups of the Gobierno Vasco/Eusko Jaurlaritza (IT834-13, IT1004- 16 and IT418-19), the Universidad del País Vasco/ Euskal Herriko Unibertsitatea (PPG17/04 and GIU18/ 163), the Geoparque de Sobrarbe, the European Regional Development Fund, and the Government of Aragón ('DGA' and 'Grupos de Referencia' E18_17R). M.M-A is supported by the "Fundação para a Ciência e a Tecnología" (grant number: SFRH/BPD/ 113130/2015). Lope Ezquerro assisted with the sedimentological interpretation of CS-41. We thank Jara Parrilla, Eduardo Medrano and Raquel Moya-Costa for joining a field expedition during a global pandemic. We thank Albert Garcia Sellés, Daniel R. Lawver, and three anonymous reviewers for their constructive comments, which improved the manuscript. We specially thank the editor, Prof. Falcon-Lang, and the journal manager, Leonard Daniel, for their understanding of our restricted access to the samples, laboratories, and fossil sites during the COVID-19 pandemic.

References

Advokaat, E.L., Van Hinsbergen, D.J.J., Maffione, M., Langereis, C.G., Vissers, R.L.M., Cherchi, A., Schroeder, R., Madani, H., Columbu, S., 2014. Eocene rotation of Sardinia, and the paleogeography of the western Mediterranean region. Earth and Planetary Science Letters 401, 183–195. https://doi.org/10.1016/j.epsl.2014.06.012

Balthasar, U., Cusack, M., Faryma, L., Chung, P., Holmer, L.E., Jin, J., Percival, I.G., Popov, L.E., 2011. Relic aragonite from Ordovician-Silurian brachiopods: implications for the evolution of calcification. Geology 39, 967–970. https://doi.org/10.1130/G32269.1

Barnolas, A., Gil-Peña, I., 2001. Ejemplos de relleno sedimentario multiepisódico en una cuenca de antepaís fragmentada: La Cuenca Surpirenaica. Boletín Geológico y Minero 112, 17–38.

Barnolas, A., Pujalte, V., 2004 (Eds). La Cordillera Pirenaica, in: Vera, J. A. (main Ed.), Geologia de España. Sociedad Geológica de España, Instituti Geológico y Minero de España, Madrid, 231–343.

Behrensmeyer, A.K., 1975. The taphonomy and paleoecology of Plio-Pleistocene vertebrate assemblages east of Lake Rudolf, Kenya. Bulletin of the Museum of Comparative Zoology 146, 473–578.

Bentham, P., Burbank, D.W., 1996. Chronology of Eocene foreland basin evolution along the western oblique margin of the South–Central Pyrenees, in: Friend, P.F., Dabrio, C.J. (Eds.), Tertiary basins of Spain, the stratigraphic record of crustal kinematics, World and Regional Geology 6, Cambridge University Press, pp. 144–152.

Bentham, P.A., 1992. The tectono-stratigraphic development of the western oblique ramp of the south-central pyrenean thrust system, northern Spain. (PhD Thesis). University of Southern California, Los Angeles, California, 253 p.

Boessenecker, R.W., Perry, F.A., Schmitt, J.G., 2014. Comparative Taphonomy, Taphofacies, and Bonebeds of the Mio-Pliocene Purisima Formation, Central California: Strong Physical Control on Marine Vertebrate Preservation in Shallow Marine Settings. PLOS ONE 9, e91419. https://doi.org/10.1371/journal.pone.0091419

Bonach, K., Malvasio, A., Matushima, E.R., Verdade, L.M., 2011. Temperature-sex determination in Podocnemis expansa (Testudinata, Podocnemididae). Iheringia. Série Zoologia 101, 151–155. https://doi.org/10.1590/S0073-47212011000200001

Bowen, G.B., Clyde,W.C., Koch, P.L., Ting, S., Alroy, J., Tsubamoto, T.,Wang,Y.,Wang,Y., 2002. Mammalian dispersal at the Paleocene-Eocene boundary. Science 295, 2062-2065.

Bravo, A.M., Buscalioni, A., Merino, L., Müller, B.G., 2003. Experimental taphonomy of avian eggs and eggshells: effects on early diagenesis. Palaeovertebrata 32, 77–95.

Buckman, J., 1860. On some Fossil Reptilian Eggs from the Great Oolite of Cirencester. Quarterly Journal of the Geological Society 16, 107–110. https://doi.org/10.1144/GSL.JGS.1860.016.01-02.11

Buscalioni, A.D., Fregenal, M.A., Bravo, A., Poyato-Ariza, F.J., Sanchíz, B., Báez, A.M., Cambra Moo, O., Martín Closas, C., Evans, S.E., Marugán Lobón, J., 2008. The vertebrate assemblage of Buenache de la Sierra (Upper Barremian of Serrania de Cuenca, Spain) with insights into its taphonomy and palaeoecology. Cretaceous Research 29, 687–710. https://doi.org/10.1016/j.cretres.2008.02.004

Canudo, J.I., 2018. The Collection of Type Fossils of the Natural Science Museum of the University of Zaragoza (Spain). Geoheritage 10, 385–392. https://doi.org/10.1007/s12371-017-0228-1

Chiappe, L.M., Coria, R.A., Dingus, L., Jackson, F., Chinsamy, A., Fox, M., 1998. Sauropod dinosaur embryos from the Late Cretaceous of Patagonia. Nature 396, 258–261. https://doi.org/10.1038/24370

Choi, S., Han, S., Kim, N. H., Lee, Y. N., 2018. A comparative study of eggshells of Gekkota with morphological, chemical compositional and crystallographic approaches and its evolutionary implications. PloS one, 13(6), e0199496. https://doi.org/10.1371/journal.pone.0199496

De Broin, F. 1977. Contribution à l'étude des Chéloniens. Chéloniens continentaux du Crétacé et du Tertiaire de France. Memoires du Muséum Nationale d'Histoire Naturelle 38, 1–366.

Broin, F. de, 1980. Les Tortues de Gadoufaoua (Aptien du Niger); aperçu sur la paléobiogéographie des Pelomedusidae (Pleurodira). Mémoires de la Société géologique de France 139, 39–46.

De Federico, A., 1981. La sedimentación de talud en el sector occidental de la cuenca paleógena de Ainsa (PhD Thesis). Universitat Autónoma de Barcelona, Barcelona, Spain, Publicaciones de Geologia 12, 271p.

Díaz-Berenguer, E. 2020. Los sirenios del Eoceno de la Cuenca de Aínsa: estudio paleobiológico de *Sobrarbesiren cardieli* (Mammalia, Sirenia). Doctoral Thesis. Universidad de Zaragoza, Zaragoza, 548 pp.

Díaz-Berenguer, E., Houssaye, A., Badiola, A., & Canudo, J. I. 2020. The Hind limbs of *Sobrarbesiren cardieli* (Eocene, Northeastern Spain) and new insights into the locomotion capabilities of the quadrupedal sirenians. *Journal of Mammalian Evolution*, 27, 649–675. https://doi.org/10.1007/s10914-019-09482-9

Díaz-Berenguer, E., Badiola, A., Moreno-Azanza, M., Canudo, J.I., 2018. First adequately-known quadrupedal sirenian from Eurasia (Eocene, Bay of Biscay, Huesca, northeastern Spain). Scientific Reports 8, 5127. https://doi.org/10.1038/s41598-018-23355-w

Dreyer, T., Corregidor, J., Arbues, P., Puigdefabregas, C., 1999. Architecture of the tectonically influenced Sobrarbe deltaic complex in the Ainsa Basin, northern Spain. Sedimentary Geology 127, 127–169. https://doi.org/10.1016/S0037-0738(99)00056-1

Gaffney, E.S., Tong, H., Meylan, P.A., 2006. Evolution of the side-necked turtles: the families Bothremydidae, Euraxemydidae, and Araripemydidae. Bulletin of the American Museum of Natural History 300, 1–700.

Garrido Mejias, A., 1968. Sobre la estratigrafia de los conglomerados de Campanué (Santa Liestra) y formaciones superiores del Eoceno (extremo occidental de la cuenca de Tremp-Graus, Pirineo Central, provincia de Huesca). Acta Geològica Hispànica 3, 39–43.

Gasca, J.M., Badiola, A., Canudo, J.I., Moreno-Azanza, M., Puértolas-Pascual, E., 2012. The fossil vertebrate asssemblage from the Pochancalo 1 site (Valanginian-Hauterivian, Villanueva de Hueva, Zaragoza, Spain). Actas de V Jornadas Internacionales sobre Paleontología de Dinosaurios y su Entorno, Salas de los Infantes, Burgos. 159–172

Gingerich, P.D., 2006. Environment and evolution through the Paleocene-Eocene thermal maximum. Trends in Ecology and Evolution 21(5), 246–253.

Hall, M.T., 1997. Sequence stratigraphy and early diagenesis: the Sobrarbe Formation , Ainsa Basin , Spain (PhD Thesis). University of Manchester, Manchester, UK.

Hayward, J.L., Dickson, K.M., Gamble, S.R., Owen, A.W., Owen, K.C., 2011. Eggshell taphonomy: environmental effects on fragment orientation. Historical Biology 23, 5–13. https://doi.org/10.1080/08912963.2010.499170

Hendrickson, J. t, Balasingam, E., 1966. Nesting beach preferences of Malayan sea turtles. Bulletin of the National Museum Singapore 33, 69–76.

Hirsch, K.F., 1985. Fossil Crocodilian Eggs from the Eocene of Colorado. Journal of Paleontology 59, 531–542.

Hirsch, K.F., 1996. Parataxonomic classification of fossil chelonian and gecko eggs. Journal of Vertebrate Paleontology. 16, 752–762. https://doi.org/10.1080/02724634.1996.10011363

Holley, J.A., Sterli, J., Basso, N.G., 2020. Dating the origin and diversification of Pan-Chelidae (Testudines, Pleurodira) under multiple molecular clock approaches. Contributions to Zoology 89, 146–174. https://doi.org/10.1163/18759866-20191419

Hooker, J.J., 1998. Mammalian faunal change across the Paleocene- Eocene transition, in: Aubry, M.-P., Lucas, S.G., Berggren,W.A. (eds.), Late Paleocene-early Eocene Climatic and Biotic Events in the Marine and Terrestrial Records. Columbia, Columbia University Press, pp. 419-441.

807 Jackson, F.D., Varricchio, D.J., Corsini, J.A., 2013. Avian eggs from the Eocene Willwood and
808 Chadron formations of Wyoming and Nebraska. Journal of Vertebrate Paleontology 33,
809 1190–1201. https://doi.org/10.1080/02724634.2013.769445
810 Jackson, F.D., Varricchio, D.J., Jackson, R.A., Walde, A.D., Bishop, G.A., 2015. Taphonomy of
811 extant desert tortoise (*Gopherus agassizii*) and loggerhead sea turtle (*Caretta caretta*)
812 nesting sites: implications for interpreting the fossil recordchelonian nest taphonomy.
813 Palaios 30, 207–223. https://doi.org/10.2110/palo.2014.048
814 Jackson, F.D., Zheng, W., Imai, T., Jackson, R.A., Jin, X., 2018. Fossil eggs associated with a
815 neoceratopsian (Mosaiceratops azumai) from the Upper Cretaceous Xiaguan
816 Formation, Henan Province, China. Cretac. Res. 91, 457–467.
817 https://doi.org/10.1016/j.cretres.2018.06.020
818 Kohring, R., 1998. Neue Schildkröten-Eischalen aus dem Oberjura der Grube Guimarota
819 (Portugal). Berliner Geowissenschaftliche Abhandlungen 28, 113–117.
820 Krefft, G., 1876. Notes on Australian animals in New Guinea with description of a new
821 species of fresh water tortoise belonging to the genus Euchelymys (Gray). *Annali del*
822 *Museuo Civico de Storia Naturale de Genova*, 1, 390–294.
823 Kuchling, G., 1999. Reproductive Behaviour, in: Kuchling, G. (Ed.), The Reproductive Biology of
824 the Chelonia, Zoophysiology. Springer Berlin Heidelberg, Berlin, Heidelberg, pp. 69–90.
825 https://doi.org/10.1007/978-3-642-80414-4_4
826 Kuntz, P. 1981. Des oeufs fossilisés. *Minéraux et Fossiles,* 7, 18–20.

827 Lawver, D.R., 2017. The evolution of reproduction within Testudinata as evidenced by the fossil
828 record. Unpublished PhD Thesis. Montana State University. 302 pp.
829 https://scholarworks.montana.edu/xmlui/handle/1/13101
830 Lawver, D.R., Jackson, F.D., 2014. A Review of the Fossil Record of Turtle Reproduction: Eggs,
831 Embryos, Nests and Copulating Pairs. Bulletin of the Peabody Museum of Natural
832 History 55, 215–236. https://doi.org/10.3374/014.055.0210
833 Lawver, D.R., Jackson, F.D., 2017. An accumulation of turtle eggs with embryos from the
834 Campanian (Upper Cretaceous) Judith River Formation of Montana. Cretaceous
835 Research 69, 90-99
836 Lawver, D.R., Rasoamiaramanana. A:H. & Werneburg I. 2015. An occurrence of fossil eggs from
837 the Mesozoic of Madagascar and a detailed observation of eggshell microstructure,
838 Journal of Vertebrate Paleontology, 35, e973030-1–e973030-6
839 https://doi.org/10.1080/02724634.2015.973030

840 Li, C., Fraser, N.C., Rieppel, O., Wu, X.-C., 2018. A Triassic stem turtle with an edentulous beak.
841 Nature 560, 476–479. https://doi.org/10.1038/s41586-018-0419-1
842 Lunsen, H.A. van, 1970. Geology of the Ara-Cinca region, Spanish Pyrenees, province of
843 Huesca, Spanish Pyrenees, procompartmentation of the Flysch basin) Phd Thesis.
844 Geologica Ultraiectina. URL http://dspace.library.uu.nl/handle/1874/217080 (accessed
845 9.10.19).
846 Marco, A., Abella-Perez, E., Tiwari, M., 2017. Vulnerability of loggerhead turtle eggs to the
847 presence of clay and silt on nesting beaches. Journal of Experimental Marine Biology
848 and Ecology 486, 195–203. https://doi.org/10.1016/j.jembe.2016.10.015
849 Mikhailov, K.E., Bray, E.S., Hirsch, K.F., 1996. Parataxonomy of fossil egg remains (Veterovata):
850 principles and applications. Journal of Vertebrate Paleontology 16, 763–769.
851 https://doi.org/10.1080/02724634.1996.10011364
852 Mortimer, J.A., 1990. The Influence of Beach Sand Characteristics on the Nesting Behavior and
853 Clutch Survival of Green Turtles (*Chelonia mydas*). Copeia 1990, 802–817.
854 https://doi.org/10.2307/1446446
855 Muñoz, J.-A., Beamud, E., Fernández, O., Arbués, P., Dinarès‐Turell, J., Poblet, J., 2013. The
856 Ainsa Fold and thrust oblique zone of the central Pyrenees: Kinematics of a curved

contractional system from paleomagnetic and structural data. Tectonics 32, 1142–1175.
Mutti, E., Tinterri, R., di Biase, D., Fava, L., Mavilla, N., Angella, S., Calabrese, L., 2000. Delta front facies associations of ancient flood-dominated fluvio-deltaic systems. Revista de la Sociedad Geologica de España 3, 165–190.
Mutti, E., Tinterri, R., Zavala, C., 1996. The importance of fluvio-deltaic systems dominated by catastrophic flooding in tectonically active basins. Memorie di Scienze Geologiche 48, 233–291.
Núñez-Lahuerta, C., Azanza, M.M., Cuenca-Bescós, G., 2019. Avian eggshell remains in the human bearing level TD6 of the Gran Dolina site (Early Pleistocene, Atapuerca, Spain). Historical Biology 33, 660–671. https://doi.org/10.1080/08912963.2019.1655009
Oser, S.E., Jackson, F.D., 2014. Sediment and eggshell interactions: using abrasion to assess transport in fossil eggshell accumulations. Historical Biology 26, 165–172. https://doi.org/10.1080/08912963.2013.814650
Packard, M.J., 1980. Ultrastructural morphology of the shell and shell membrane of eggs of common snapping turtles (Chelydra serpentina) - Packard - 1980 - Journal of Morphology - Wiley Online Library. Journal of Morphology 165, 187–204.
Packard, M.J., Hirsch, K.F., Iverson, J.B., 1984. Structure of shells from eggs of kinosternid turtles. Journal of Morphology 181, 9–20. https://doi.org/10.1002/jmor.1051810103
Pérez-García, A., 2017. The Iberian fossil record of turtles: an update. J Iber Geol 43, 155–191. https://doi.org/10.1007/s41513-017-0016-4
Pérez-García, A., 2016. A new turtle confirms the presence of Bothremydidae (Pleurodira) in the Cenozoic of Europe and expands the biostratigraphic range of Foxemydina. Sci Nat 103, 50. https://doi.org/10.1007/s00114-016-1375-y
Pérez-García, A., Díaz-Berenguer, E., Badiola, A., Canudo, J.I., 2021. An unexpected finding: identification of the first complete shell of the Franco-Belgian middle Eocene littoral pleurodiran turtle *Eocenochelus eremberti* in Spain. Historical Biology 33, 527–533. https://doi.org/10.1080/08912963.2019.1644330
Pérez-García, A. 2018. New genera of Taphrosphyina (Pleurodira, Bothremydidae) for the French Maastrichtian '*Tretosternum*' *ambiguum* and the Peruvian Ypresian '*Podocnemis*' *olssoni*. Historical Biology 32, 555–560. https://doi.org/10.1080/08912963.2018.1506779.
Pérez-García, A., Lapparent de Broin, F. de, Murelaga, X., 2017. The *Erymnochelys* group of turtles (Pleurodira, Podocnemididae) in the Eocene of Europe: New taxa and paleobiogeographical implications. *Palaeontologia Electronica* 20.1.14Ahttps://doi.org/10.26879/687
Pérez-García, A., Murelaga, X., Lalueza, J.C., Badiola, A., Ester, D.-B., 2013. Presence of several clades of continental turtles in the Lutetian (Middle Eocene) of the Sobrarbe Formation (Ainsa Basin, south-central Pyrenees, northeast Spain). Geologica Belgica 16/4, 311–319.
Pérez-García, A., Smith, T., 2017. Identification of the African–European *Erymnochelys* group (Pleurodira, Podocnemididae) in the Belgian fossil record: first finding of *Eocenochelus eremberti* outside its type locality. Fossil Record 20, 245–251. https://doi.org/10.5194/fr-20-245-2017
Pritchard, P.C.H., 1979. Encyclopedia of turtles. TFH New Jersey, Estados Unidos.
Rosenbaum, G., Lister, G.S., Duboz, C., 2002. Relative motions of Africa, Iberia and Europe during Alpine orogeny. Tectonophysics 359, 117–129. https://doi.org/10.1016/S0040-1951(02)00442-0
Schleich, H.H., Kästle, W., Dyck, M.-C.G., 1988. Paläogene Eischalenreste von Hainin (Belgien). Paläont. Z. 62, 133–146. https://doi.org/10.1007/BF02989839
Stancyk, S.E., Ross, J.P., 1978. An Analysis of Sand from Green Turtle Nesting Beaches on Ascension Island. Copeia 1978, 93–99. https://doi.org/10.2307/1443827

909 Solé, F., Smith, Th., 2013. Dispersal of placental carnivorous mammals (Carnivoramorpha,
910 Oxyaenodonta & Hyaenodontida) near the Paleocene-Eocene boundary: a climatic and
911 almost worldwide story. Geologica Belgica 16/4, 254-261.
912 Ubeid, K., 2008. El Delta del Sobrarbe (Eoceno) en el flanco E del sinclinal de Santa María del
913 Buil (cuenca de Aínsa, Pirineos Centrales-meridionales, N de España): facies,
914 arquitectura y su relación con los sistemas marinos profundos (PhD Thesis).
915 Universidad de Oviedo, Oviedo, Spain, 176p.
916 Vila, B., Jackson, F.D., Fortuny, J., Sellés, A.G., Galobart, À., 2010. 3-D Modelling of
917 Megaloolithid Clutches: Insights about Nest Construction and Dinosaur Behaviour.
918 PLOS ONE 5, e10362. https://doi.org/10.1371/journal.pone.0010362
919 Wang, P.L., Jackson, F.D., Varricchio, D.J., 2014. Nest taphonomy of common terns (Sterna
920 hirundo) on Poplar Island, Chesapeake Bay, Maryland. Historical Biology 26, 155–164.
921 https://doi.org/10.1080/08912963.2013.798317
922 Winkler, J.D., 2006. Testing phylogenetic implications of eggshell characters in side-necked
923 turtles (Testudinata: Pleurodira). Zoology 109, 127–136.
924 https://doi.org/10.1016/j.zool.2005.12.003.
925 Zelenitsky D. K, Therrien, F., Joyce, W.G., Brinkman D.B., 2008. First fossil gravid turtle provides
926 insight into the evolution of reproductive traits in turtles. Biology Letters 4, 715–718
927 http://doi.org/10.1098/rsbl.2008.0395
928

929 Table 1. Microfossil contents from three random samples of rock from the CS-41 fossil site. All
930 samples come from Facies 3. The location of each sample is shown in Supplementary
931 Figure 1.

	CS41-C14 (21 kg)		CS41-C16/17 (12 kg)		CS41-C19/20 (14 kg)	
ELEMENTS	**#**	**#/kg rock**	**#**	**#/kg rock**	**#**	**#/kg rock**
Eggshells	6777	**322.7**	1596	**133**	3691	**263.64**
Unidentified vertebrate bones and splinters	3758	**178.9**	488	**40.666**	569	**40.64**
Crocodylomorph teeth	8	**0.38**	0	**0**	5	**0.357**
Chondrichthyan teeth	4	**0.19**	0	**0**	2	**0.14**
Chondrichthyan dermal denticles	4	**0.19**	2	**0.1666**	7	**0.5**
Osteichthyan teeth	1	**0.05**	0	**0**	0	**0**
Unidentified tooth fragments	4	**0.19**	0	**0**	0	**0**
Otoliths	52	**2.47**	59	**4.916**	62	**4.43**
Gastropods	61	**2.9**	172	**14.33**	212	**15.14**
Bivalves	10	**0.47**	1	**0.083**	4	**0.28**
Echinoderms	0	**0**	1	**0.083**	0	**0**
Indeterminate calcareous fossils	56	**2.66**	18	**1.5**	24	**1.714**
Charophyte remains	15	**0.71**	1	**0.083**	1	**0.07**
Unidentified plant remains	90	**4.28**	0	**0**	0	**0**
Foraminifera	1	**0.05**	0	**0**	2	**0.14**
TOTAL REMAINS	10841	**516.2**	2337	**194.8276**	4579	**327.051**

932

933 Table 2. Comparison of the number of eggshell fragments per kilogram of processed sediment
934 in selected eggshell localities.

Locality	Palaeoenvironment	Eggshells/ rock kg	Age	References
Buenache de la Sierra	Fluvial, alluvial plain	2.4	Barremian	(Buscalioni et al., 2008)
Pochancalo 1	Fluvial, crevasse splay	3.5	Valanginian	(Gasca et al., 2012)
Colladico Blanco 2	Lacustrine, attritional	13	Barremian	(Gasca et al., 2012)
Cuesta Corrales 2	Lacustrine, nest debris	107	Barremian	Unpublished
CS-41	Deltaic, intertidal	212	Lutetian	This work

935

936

Figure Headings

Figure 1. Geographical and geological setting of the Castejón de Sobrarbe-41 (CS-41) fossil site. A, Geological map of the Ainsa Basin, with the location of the CS-41 fossil site. B, Palaeogeographic location of the Iberian Peninsula during the Lutetian. C, Stratigraphic log and facies interpretation of the Castejón de Sobrarbe section, comprising the upper part of the Sobrarbe Formation and including the location of the CS-41 fossil site. Grain size abbreviations: C, clay; s, silt; fS, fine sand; mS, medium sand; cS, coarse sand; G, gravel. D, Relative abundance of microfossil remains recovered in the CS-41 fossil site. Relative abundances with respect to the total remains recovered and with respect to the vertebrate remains.

Figure 2. Sedimentology of the CS-41 fossil bonebed. A, View of the bonebed profile at y=900. B, schematic drawing of A, showing the three facies composing the sedimentary sequence: Facies 1, low-angle crevasse-splay deposit. Facies 2, energetic channel infill with few fossils. Facies 3, highly fossiliferous, less energetic, channel infill. Note the presence of two sections of sirenian ribs in the process of collection. C, View of the bonebed profile at x=210, y=700. D, sedimentological log of the CS-41 bonebed at x=210, y=700, with grain size distribution diagrams for each facies.

Figure 3. Secondary electron microphotographs of Testudoolithidae indet. eggshells from the CS-41 fossil site. A-C, radial sections. Note the presence of acicular calcite crystal phantoms forming the shell units in A, which are completely replaced by rhombohedra in B and C, suggesting different degrees of recrystallization of the original aragonite radial ultrastructure. D, E, outer surfaces, showing well-preserved compactituberculate ornamentation (D) and abraded outer surface (E). White square signals a node cluster, formed by three highly interlocked shell units. F, inner surface, showing tightly abutted shell units with cratered bases of the shell units and preserved acicular crystals radiating out from the primary spherites. G, close-up of a deformed shell unit, squeezed between neighbouring units during eggshell growth. H, twin primary spherites. A, MPZ 2021/56; B, MPZ 2021/55; C, MPZ 2021/58; D, MPZ 2021/56; E, MPZ 2021/57. F, MPZ 2021/57, G MPZ 2021/56. H, MPZ 2021/57.

Figure 4. Petrographic microscope photographs (A-D) and electron backscatter diffraction maps (E-G) of radial thin sections of Testudoolithidae indet. eggshells from the CS-41 fossil site. A, B, MPZ 2021/78 in parallel-polarized light (A) and cross-polarized light (B), showing barrel-shaped shell units with a radial texture that is a relic of the original aragonite crystals (A), contrasting with the large sub-euhedral calcite crystals (B). Note the straight pore channels with funnel-

shaped pore openings (arrow). C, D, MPZ 2021/77 in parallel-polarized light (C) and cross-polarized light (D). Eggshell with a diagenetically flattened outer surface due to severe recrystallization. Note that some of the large euhedral crystals cross between shell units (arrow). E, MPZ 2021/80 phase composition map, with -3m calcite mapped in yellow, and Pmcn aragonite mapped in red. Note that the small size of the red areas suggests that these relics may be indexing artefacts. F, MPZ 2021/80 inverse pole figure map, showing the relative orientation of the different crystallographic domains, coloured according to the orientation of the c axis of each crystal (see pole figure). Note that the main orientation is tilted 60 degrees with respect to the outward eggshell growth direction. G, MPZ 2021/80 grain boundary map showing the relative misorientation between neighbouring crystal domains (green 5°–10°, blue 10°–20° and yellow > 20°).

Figure 5. Plastra of four specimens of *Eocenochelus eremberti* (Pleurodira, Erymnochelyini) from the CS-41 site, in ventral view. A, close-up of the anterior plastral lobe of the complete shell MPZ 2019/263 (for the complete figuration of this specimen see Pérez-García et al., 2021). B-D, previously unpublished specimens, corresponding to the individuals MPZ 2021/83 (B), MPZ 2021/81 (C), MPZ 2021/82 (D). The scute margins are represented by thicker grey lines, and those corresponding to the plates by narrower black lines. Abbreviations for the plates (in lowercase): ent, entoplastron; ep, epiplastron; hp, hypoplastron; hy, hyoplastron; ms, mesoplastron; xi, xiphiplastron. Abbreviations for the scutes (in uppercase): AB, abdominal; AN, anal; FE, femoral; GU, gular; HU, humeral; INT, intergular; MA, marginal; PC, pectoral.

Figure 6. A, Reconstruction of the depositional environment of the CS-41 site within the deltaic plain, showing the fossil inputs from the different environments in the Sobrarbe Deltaic Complex. B, Biostratinomic genesis of the eggshell accumulation. Eggshells were laid by *Eocenochelus* females in sandy deposits along the delta mouth (B1). The nests were exhumed by storm events (B2) that washed over the deltaic plain and deposited them in an abandoned channel (B3), together with exhumed sirenian and turtle remains.

Supplementary Figure 1. Map of the CS-41 site, showing the location of the most relevant macrovertebrate remains. Key specimens are drawn. Black dots represent specimens of less than 10 cm in length. The channel morphology of the deposit is evidenced by the concentration of remains within an area one metre wide by at least six metres long, with a north to south direction, bending gently towards the east. *Eocenochelus eremberti* remains are coloured green. Red dot marks the location of the profile in Figure 2CD. Orange squares show the approximate location of the microfossil samples studied.

Supplementary Figure 2. Cryptodira indet. isolated partial plates collected in the CS-41 fossil site. A, MPZ 2021/87; B, MPZ 202188.

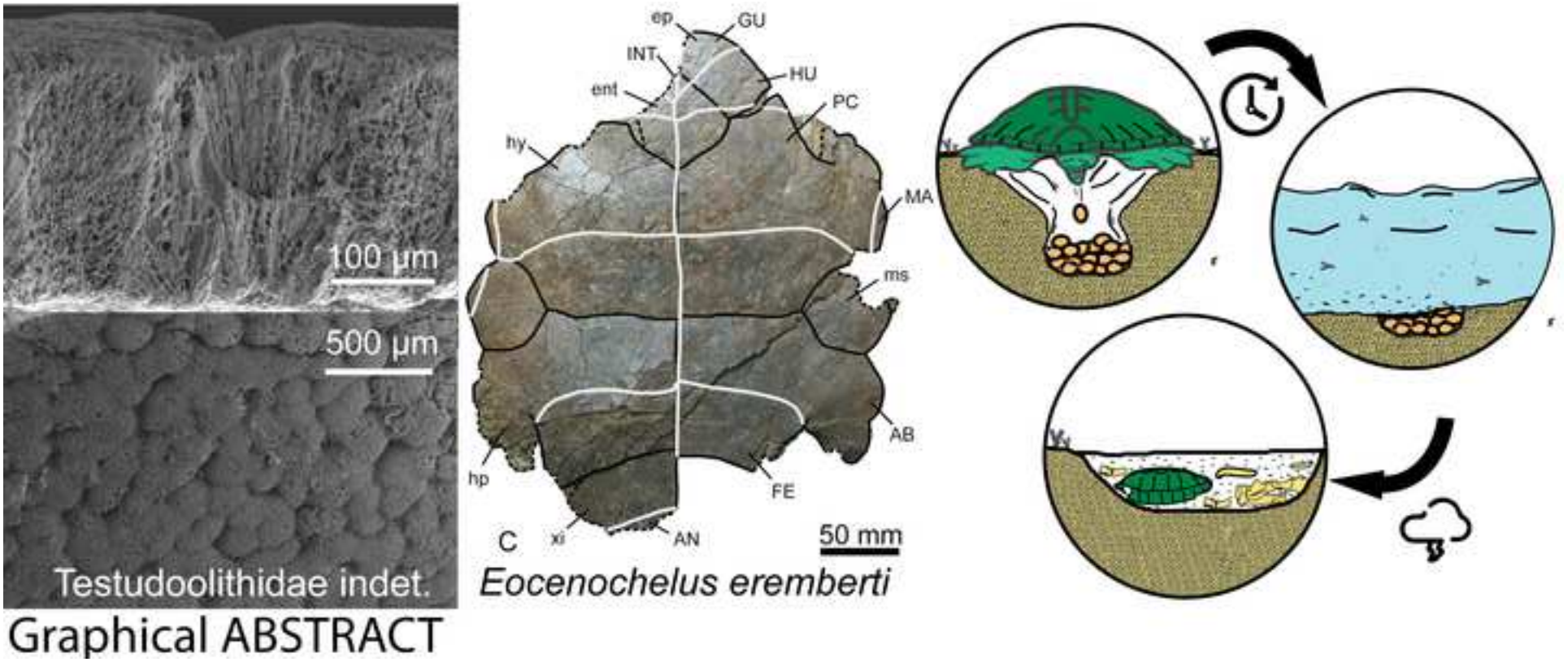

Graphical ABSTRACT

Figure 1

Click here to access/download;Figure;Figure final_Figure 1.tif

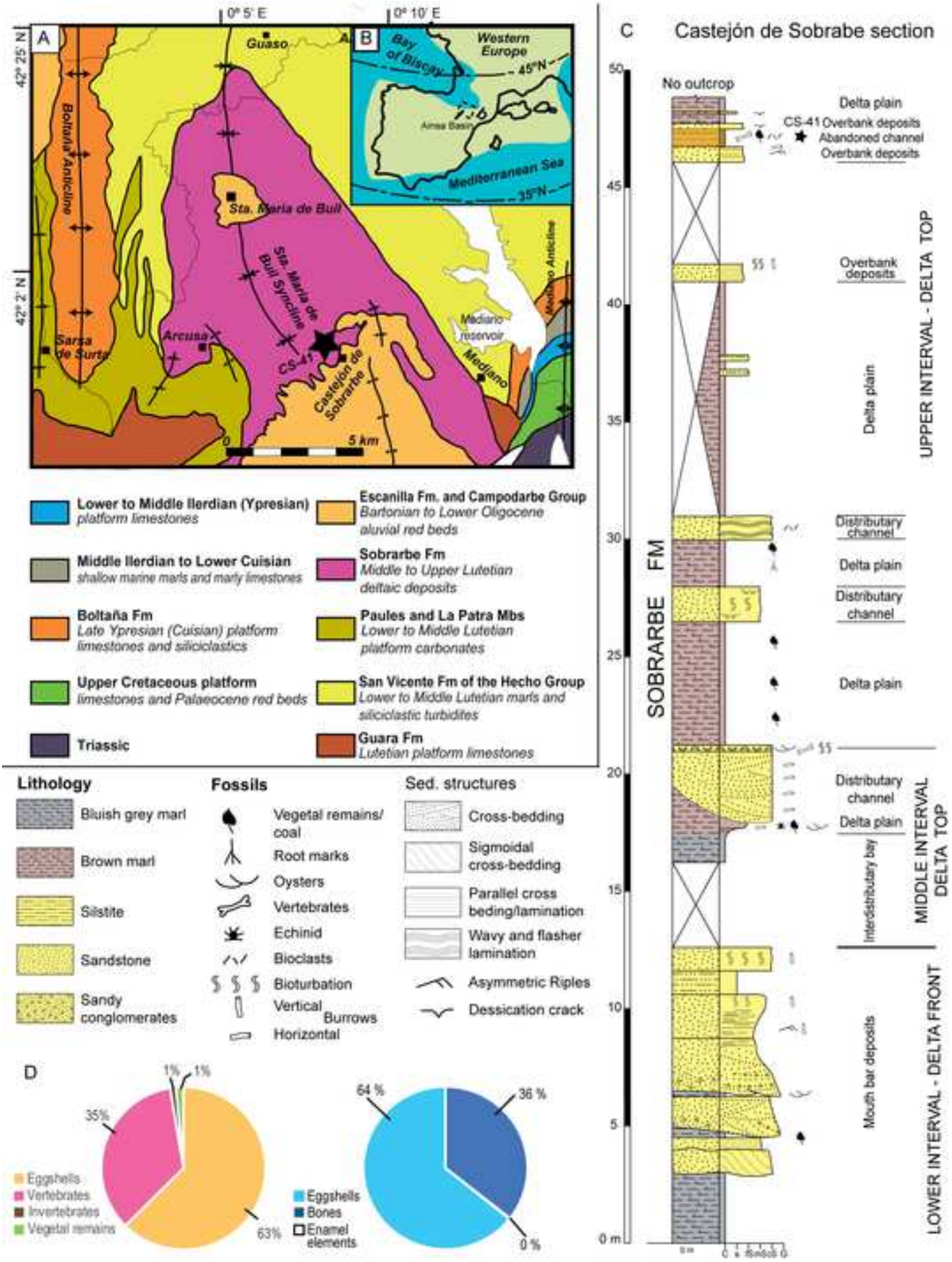

Figure 2

Click here to access/download;Figure;Figure final_Figure 2.tif

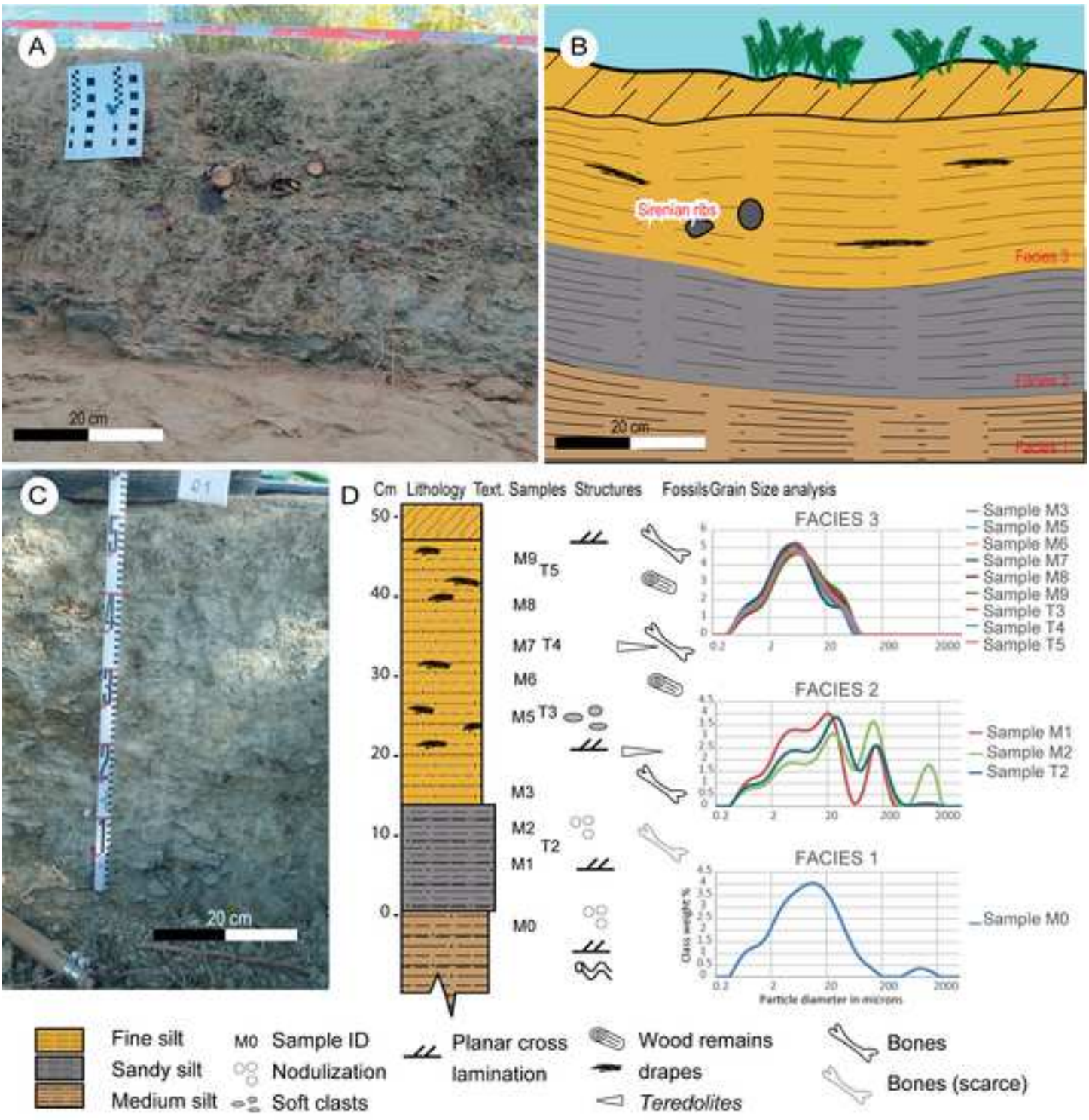

Figure 3

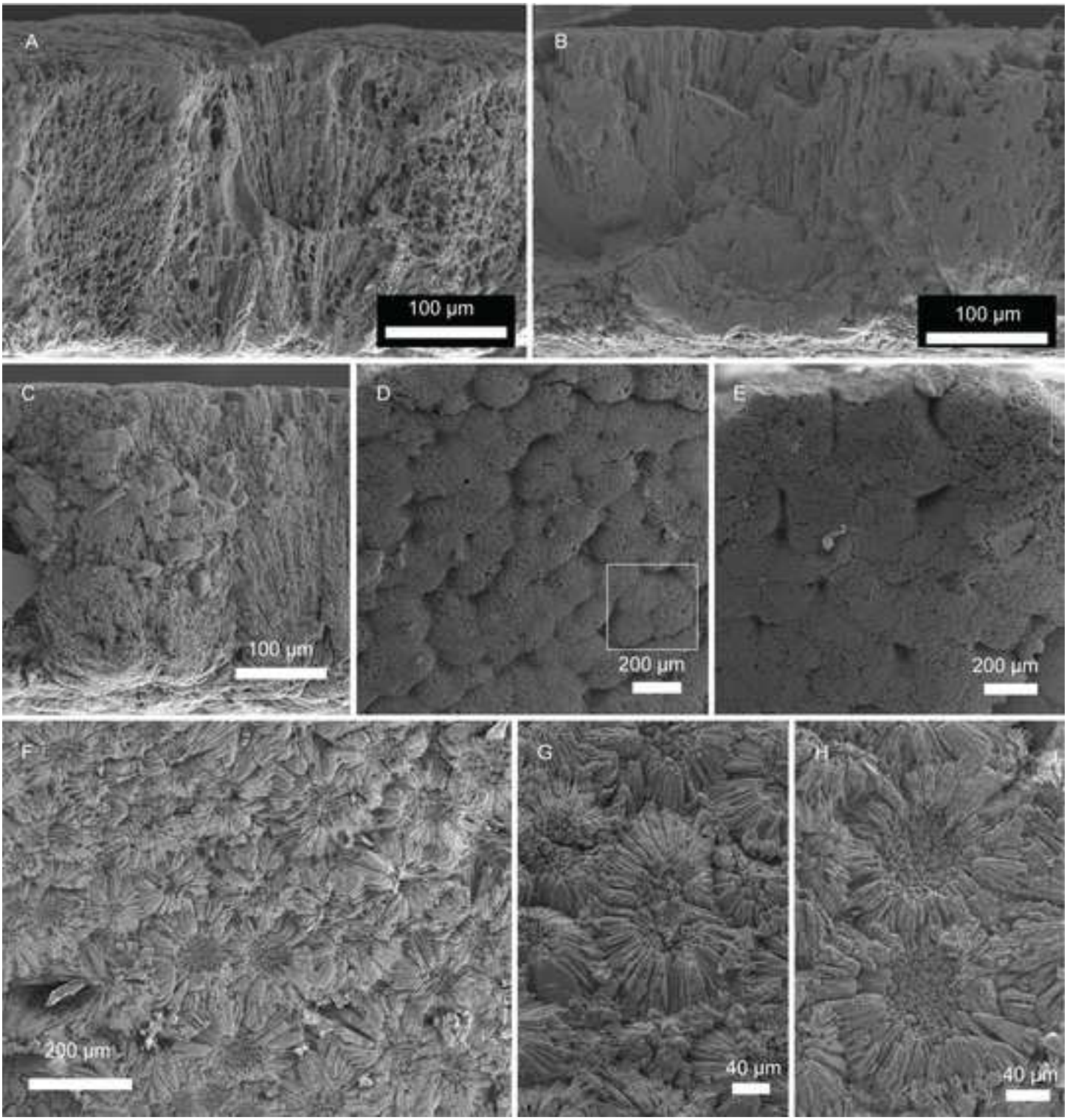

Figure 4

Click here to access/download;Figure;Figure final_Figure 4.tif

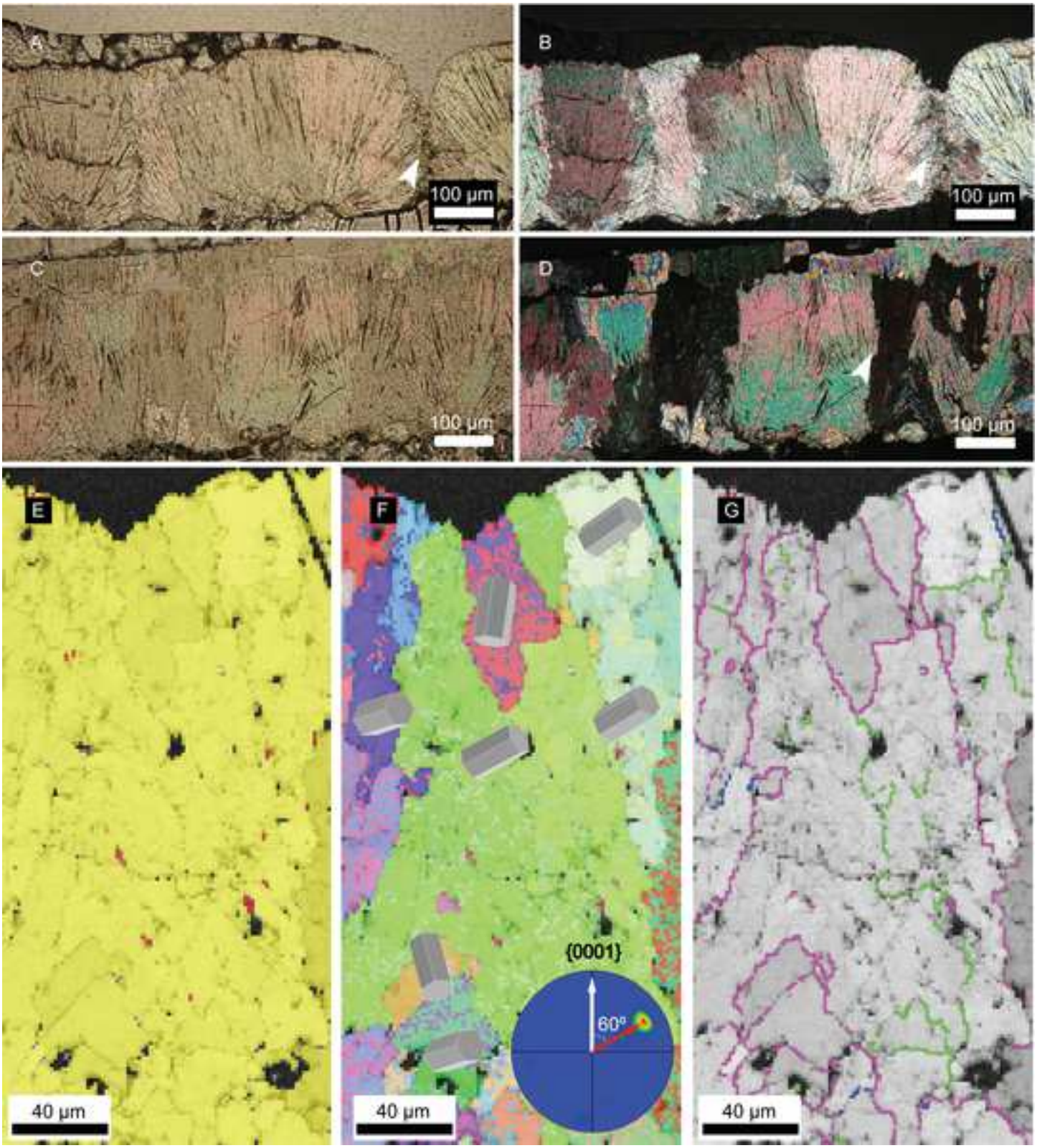

Figure 5

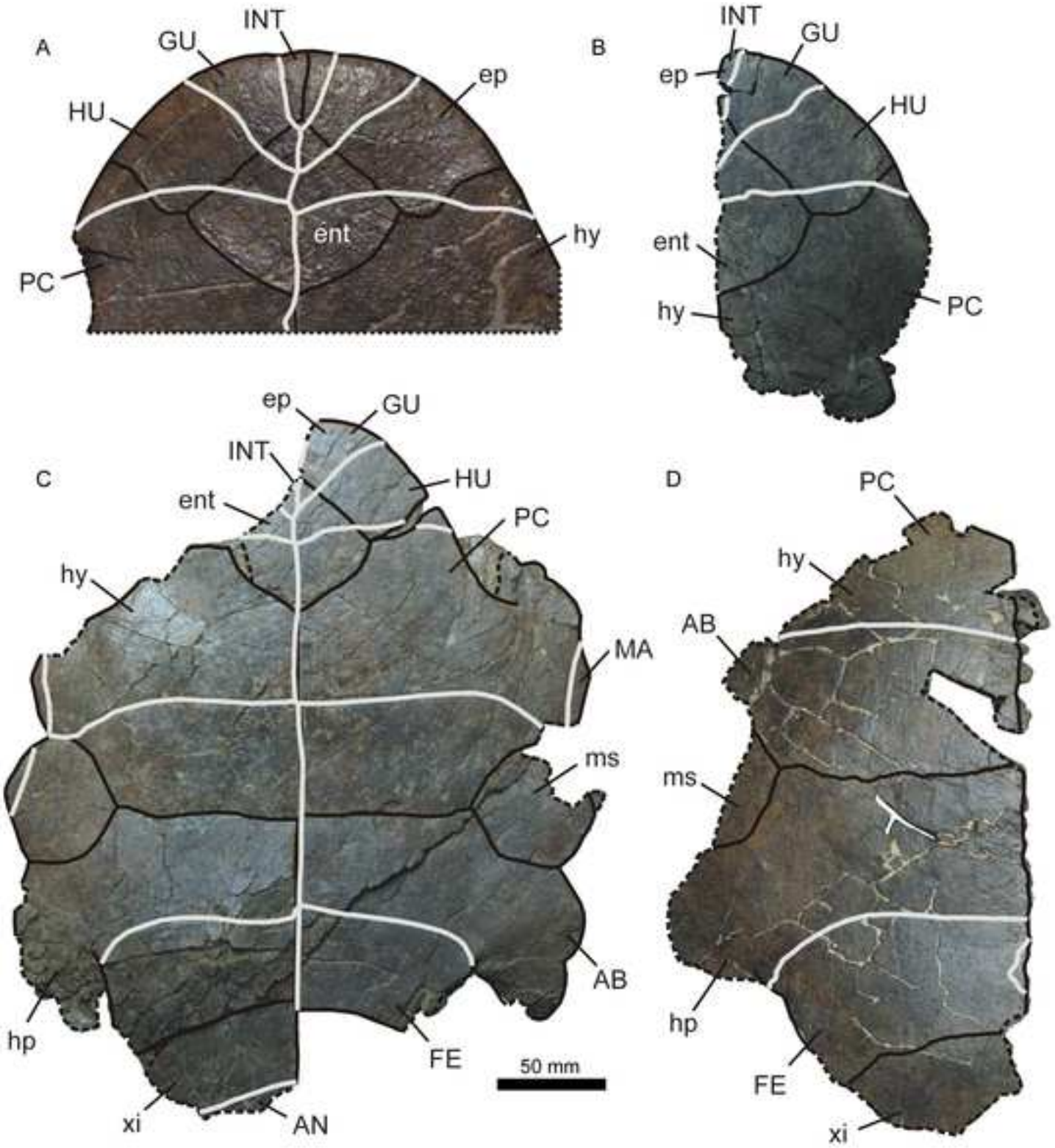

Figure 6

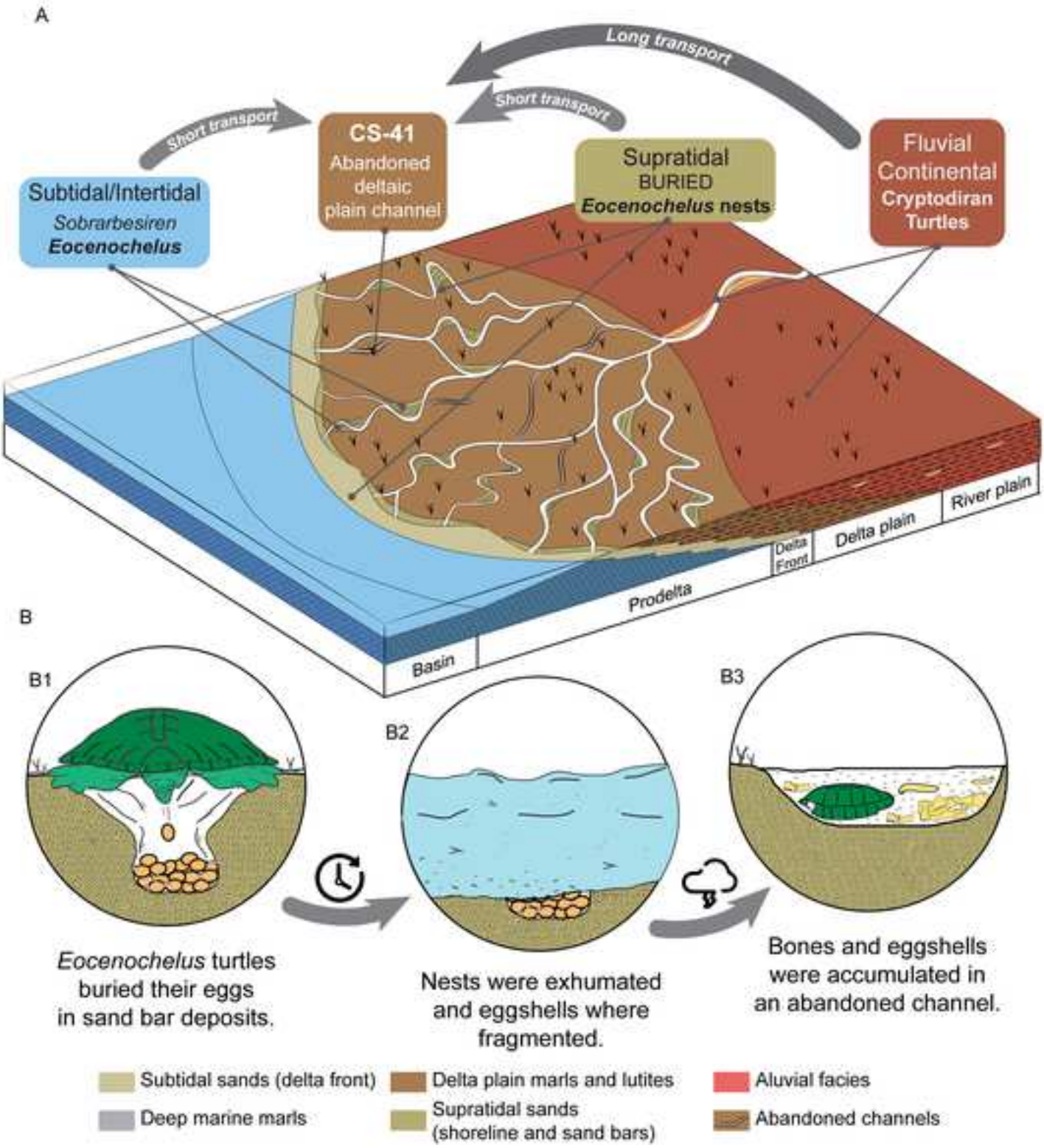

Supplementary Figure 1

Click here to access/download;Figure;Figure final_Supplementary Figure 1.tif

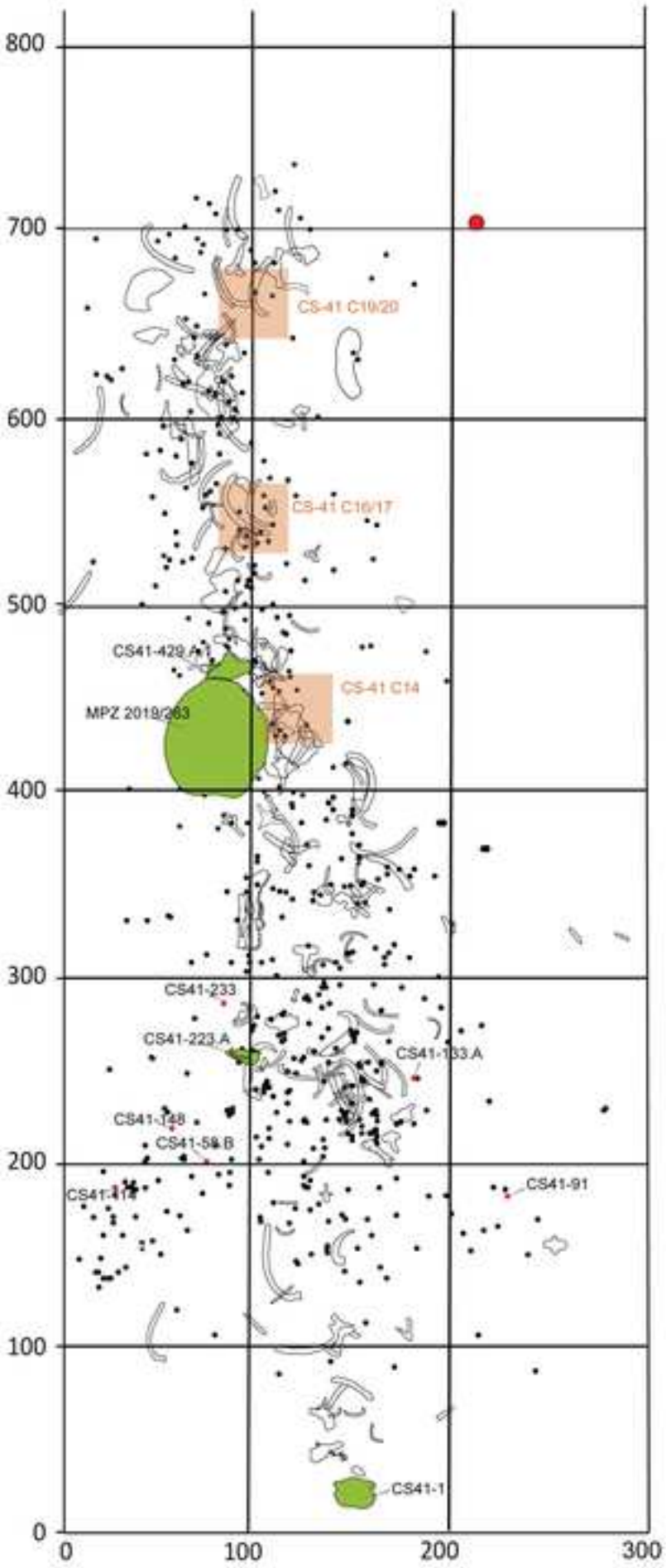

Supplementary Figure 2

Click here to access/download;Figure;Figure final_Supplementary Figure 2.tif

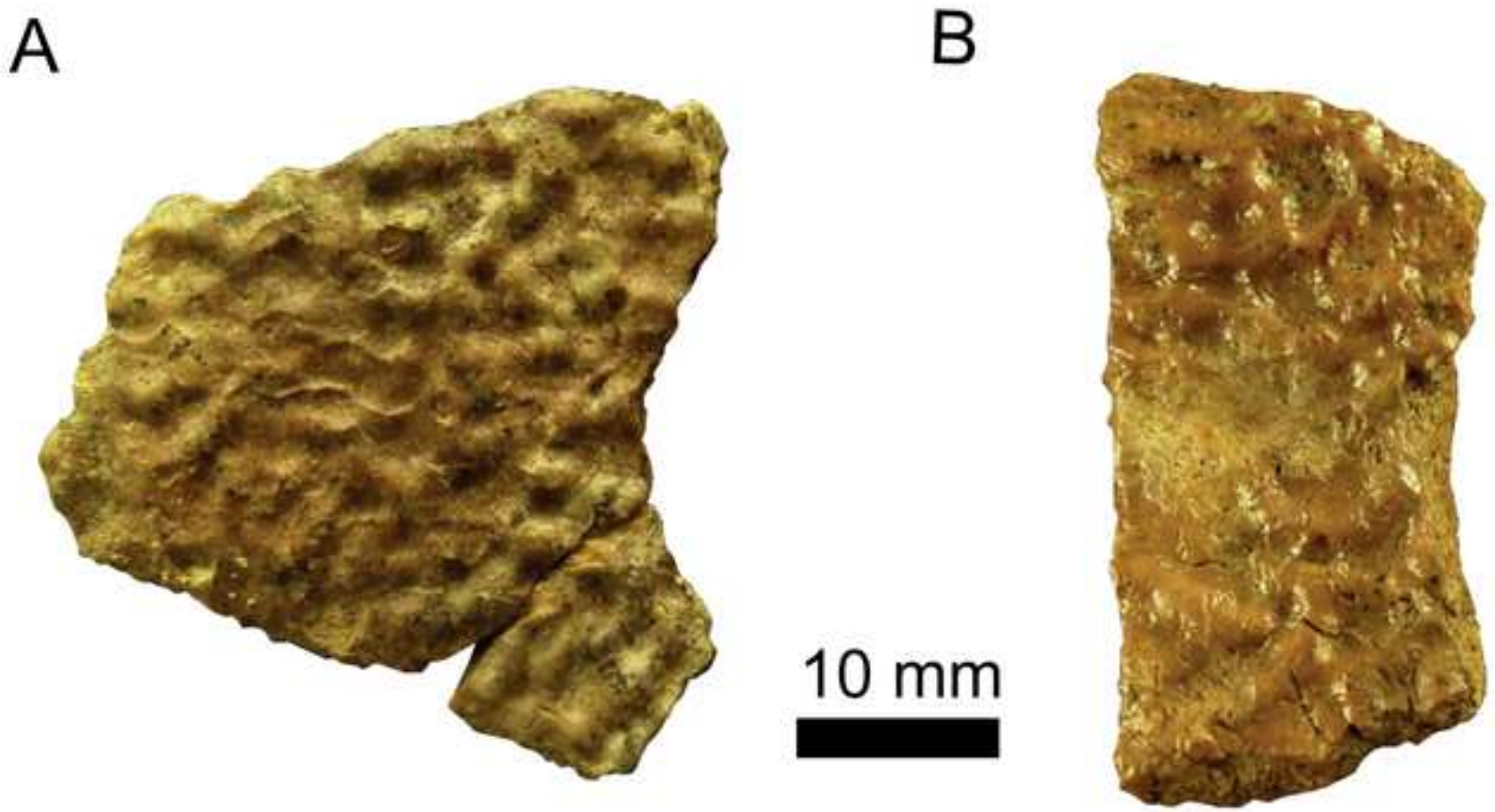

All authors have participated in (a) conception and design, or analysis and interpretation of the data; (b) drafting the article or revising it critically for important intellectual content; and (c) approval of the final version.

This manuscript has not been submitted to, nor is under review at, another journal or other publishing venue.

The authors have no affiliation with any organization with a direct or indirect financial interest in the subject matter discussed in the manuscript.

All materials were collected under the local regulations (Direción General de Patrimonio Cultural, Gobierno de Aragón). Fossils are housed in the Museo de Ciencias Naturales de la Universidad de Zaragoza (MPZ).